ELSEVIER

Contents lists available at ScienceDirect

## Ore Geology Reviews

journal homepage: www.elsevier.com/locate/oregeorev



# Microtextural evidence for the recrystallization of opal-A to quartz in epithermal veins: A case study from the McLaughlin deposit, California

Garrett D. Gissler <sup>a</sup>, Thomas Monecke <sup>a,\*</sup>, T. James Reynolds <sup>a,b</sup>, Mario A. Guzman <sup>a,c</sup>, Eric T. Ellison <sup>d</sup>, Ross Sherlock <sup>e</sup>

- <sup>a</sup> Center to Advance the Science of Exploration to Reclamation in Mining, Department of Geology and Geological Engineering, Colorado School of Mines, 1516 Illinois Street. Golden. CO 80401. USA
- <sup>b</sup> FLUID INC., 1401 Wewatta St. #PH3, Denver, CO 80202, USA
- <sup>c</sup> United States Geological Survey, Denver Federal Center, Denver, CO 80225, USA
- d Department of Geological Sciences, University of Colorado Boulder, 2200 Colorado Avenue, Boulder, CO 80309, USA
- e Mineral Exploration Research Centre, Harquail School of Earth Sciences, Laurentian University, 935 Ramsey Lake Road, Sudbury, ON P3E 2C6, Canada

#### ARTICLE INFO

#### Keywords: Epithermal deposits Opal-A recrystallization Quartz textures Petrography

## ABSTRACT

High-grade ores in low-sulfidation epithermal deposits commonly consist of banded veins containing quartz as the most abundant gangue mineral. Previous studies suggested that at least some of the quartz has formed as a product of recrystallization from a noncrystalline silica precursor. Detailed petrographic studies confirm that high-grade veins from the <2.2 Ma McLaughlin deposit in California were originally entirely composed of opal-A<sub>G</sub>. The noncrystalline silica is isotropic in crossed-polarized light and consists of compacted microspheres that are up to several micrometers in size. In many bands of the high-grade veins, the thermodynamically unstable  $opal-A_G$  has matured to quartz. The recrystallization of the noncrystalline silica resulted in the development of quartz and ore textures that mask the original conditions of vein formation. Incipient recrystallization of the opal-A<sub>G</sub> caused the formation of lepispheres consisting of opal-CT as well as the development of concentrically banded silica spheres. Continued maturation led to the growth of elongated quartz crystals or complexly shaped quartz aggregates in the cores of the concentrically banded silica spheres. Amalgamation of quartz crystals caused the development of mosaic quartz or flamboyant quartz. Ripening produced large prismatic quartz crystals, which are characterized by zones of feathery appearance. Fluid inclusions within the quartz formed through recrystallization are typically highly irregular in shape and show inconsistent liquid-to-vapor volumetric proportions, but assemblages with consistent ratios are also present. Bands rich in fluid inclusions occurring along former recrystallization fronts in prismatic quartz crystals resemble growth zones in zonal quartz. Recrystallization of the silica matrix resulted in grain coarsening of the ore minerals and encapsulation of ore minerals by quartz. In areas where recrystallization of the noncrystalline silica proceeded to completeness, the quartz textures could be easily misinterpreted to indicate that quartz growth occurred in open space with the ore minerals infilling vug spaces. Correct recognition of recrystallization textures has significant implications for paragenetic investigations on vein material from epithermal deposits as well as the design of fluid inclusion studies.

## 1. Introduction

Low-sulfidation epithermal deposits are a significant source of gold (Lipson, 2014). The deposits form within hundreds of meters from the paleosurface from hydrothermal liquids having temperatures of up to 250 °C. The ore-forming liquids are dilute aqueous solutions with low (<2 mol %) CO<sub>2</sub> contents (Hedenquist et al., 2000; Simmons et al.,

2005). In many low-sulfidation epithermal deposits, precious metal enrichment is confined to banded quartz veins that have formed along faults that control the upflow of the hydrothermal liquids to the surface (Rowland and Simmons, 2012). Ore minerals are hosted in certain bands within the veins suggesting that the deposition of metals occurred intermittently during vein formation (Hedenquist et al., 2000; Sanematsu et al., 2006; Shimizu, 2014; Tharalson et al., 2019, 2023; Zeeck

E-mail address: tmonecke@mines.edu (T. Monecke).

https://doi.org/10.1016/j.oregeorev.2024.106105

<sup>\*</sup> Corresponding author.

et al., 2021). Deposition of the ore minerals in these bands is widely attributed to metal supersaturation associated with vapor loss from the ascending hydrothermal liquids (Drummond and Ohmoto, 1985; Brown, 1986; Christenson and Hayba, 1995; Simmons and Browne, 2000; Taksavasu et al., 2018; Tharalson et al., 2019, 2023; Zeeck et al., 2021).

In contrast to banded quartz veins in low-sulfidation epithermal deposits, scales in active geothermal systems are composed of opal- $A_G$ , which is a noncrystalline silica phase consisting of microspheres that range up to several micrometers in diameter (cf. Smith, 1998). Scales composed of this noncrystalline silica phase occur within production wells (Henley and Brown, 1985; Brown, 2011; Chambefort and Stefánsson, 2020) and geothermal surface installations (Reyes et al., 2002; Smith et al., 2003; Raymond et al., 2005; Taksavasu et al., 2018; van den Heuvel et al., 2018). The difference in mineralogical composition between banded veins in epithermal deposits and scales in geothermal wells may be explained by the fact that opal- $A_G$  is thermodynamically unstable and recrystallizes to quartz over time (Herdianita

et al., 2000; Campbell et al., 2001; Lynne and Campbell, 2004; Lynne et al., 2005; Rodgers et al., 2004).

Dong et al. (1995) proposed that recrystallization of a noncrystalline silica precursor results in the development of distinct quartz textures. Following the original suggestion of Lovering (1972), Dong et al. (1995) hypothesized that mosaic quartz, which is microcrystalline quartz characterized by highly irregular and interpenetrating grain boundaries, is such a product of recrystallization. Mosaic quartz is one of the most common quartz textures in epithermal deposits of diverse ages (Saunders, 1990, 1994; Scott and Watanabe, 1998; Dong et al., 1995; Moncada et al., 2012; Taksavasu et al., 2018; Tharalson et al., 2019, 2023; Zeeck et al., 2021). Furthermore, Sander and Black (1988) and Dong et al. (1995) speculated that flamboyant quartz is also a recrystallization texture and does not form through precipitation of quartz in open space.

This contribution focuses on the petrographic study of opaline vein material from McLaughlin in California, which is an unusually wellpreserved low-sulfidation epithermal deposit that has not been

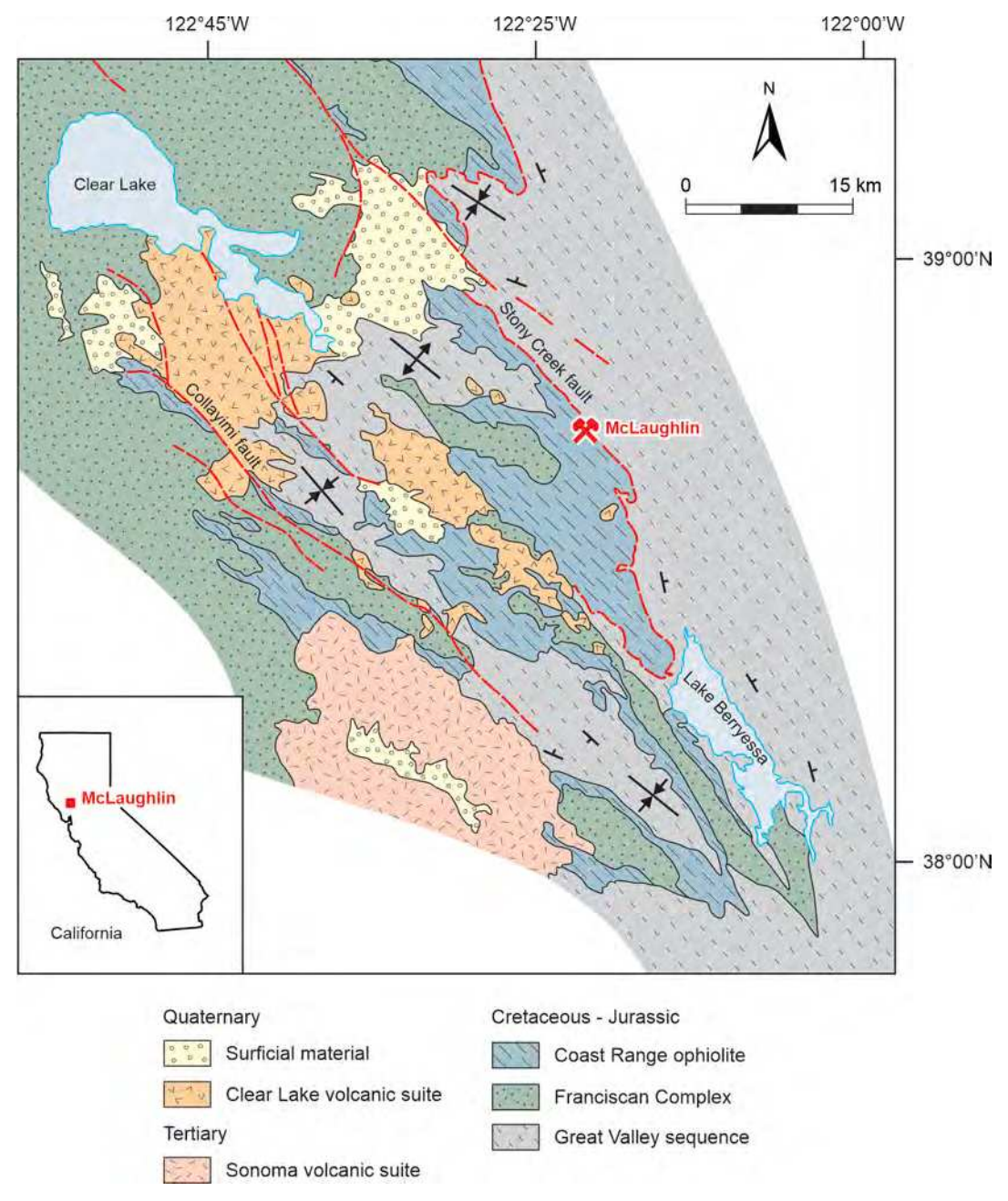


Fig. 1. Geologic setting of the McLaughlin deposit in the Clear Lake area of California. Modified from Sherlock (2005).

subjected to tectonic or metamorphic overprint (Sherlock et al., 1995). Opaline veins from McLaughlin still contain relict microspherical opal-  $A_{\rm G}$  (Monecke et al., 2023; Tharalson et al., 2023), which has only partially recrystallized to quartz, allowing the identification and study of the textures associated with this transformation. It is shown here that the recrystallization of noncrystalline silica can result in complex textural relationships, which can be easily misinterpreted to indicate that mineral deposition occurred in open space. Accurate interpretation of the textural relationships has significant implications for paragenetic studies as well as fluid inclusion investigations of epithermal deposits.

#### 2. Geology

In 1978, Homestake Mining Company discovered the McLaughlin deposit, which is located  $\sim$ 120 km north of San Francisco in the Clear Lake area in California (Fig. 1). Open pit mining was conducted from

1983 to 1996 at an average grade of 4.49 g per metric ton Au (Sherlock and Lehrman, 1995; Sherlock et al., 1995). Prior to mining, the total resource of the deposit was calculated at 3.5 million ounces of Au contained within 24.3 million tonnes of ore (Sherlock and Lehrman, 1995). Precious metals enrichment occurred from the surface to a depth of ~350 m (Sherlock et al., 1995).

The Pleistocene (<2.2 Ma; Lehrman, 1986) McLaughlin low-sulfidation epithermal deposit is located along the moderately northeast dipping Stoney Creek fault, which separates serpentinized ultramafic and mafic rocks of the Middle Jurassic Coast Range ophiolite in the southwest from hangingwall mudstone of the Late Jurassic to Early Cretaceous Great Valley sequence to the northeast (Tosdal et al., 1993). The main ore body comprised a pipe-like sheeted vein complex formed in a dilatant zone between basalts and a mélange of sedimentary rocks and serpentinite (Fig. 2). The sheeted vein complex is up to 100 m in width and is composed of centimeter to meters wide, crosscutting

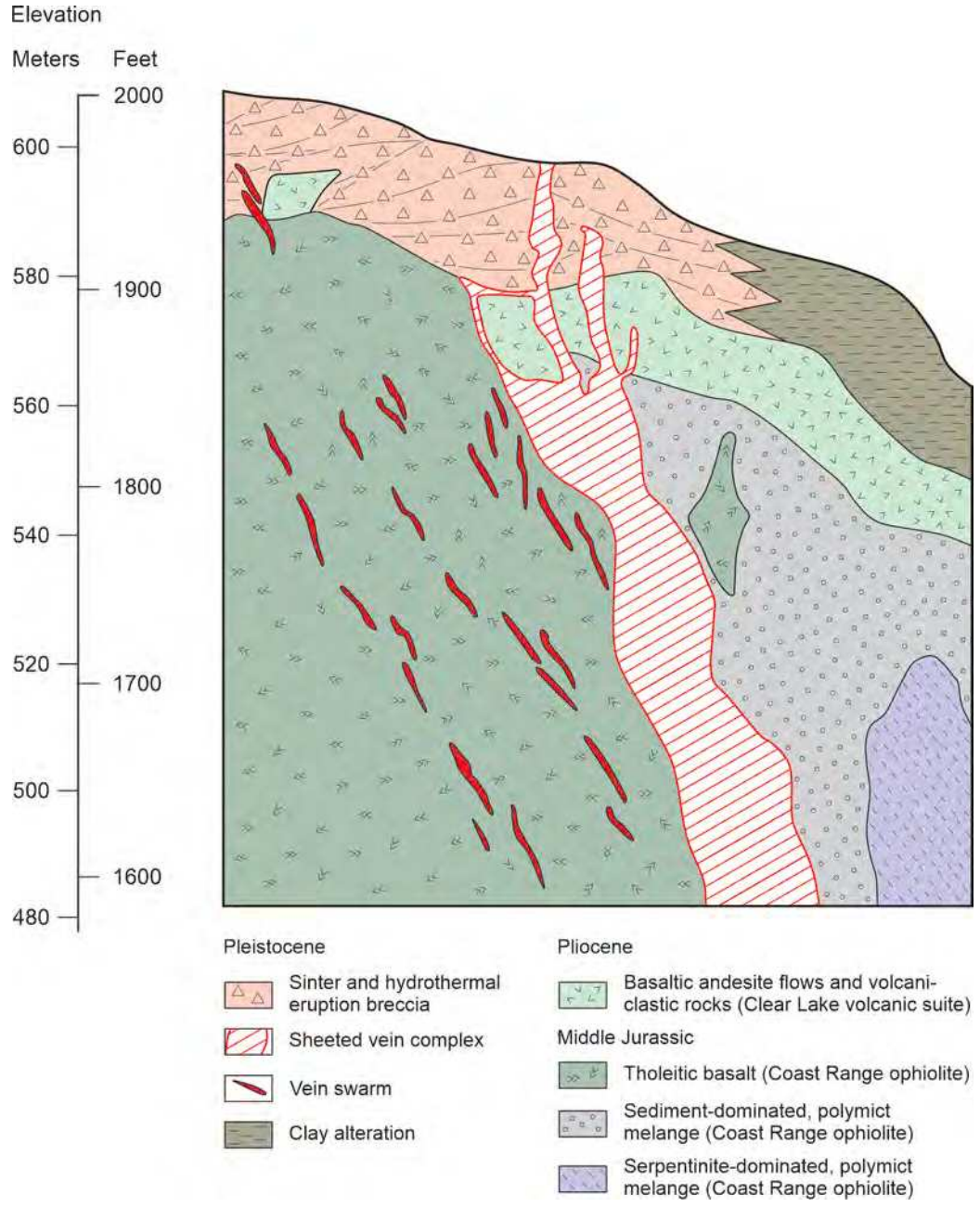


Fig. 2. Cross-section through the sheeted vein complex at the McLaughlin deposit. Modified from Sherlock et al. (1995).

opaline veins (Fig. 3a; Tosdal et al., 1993; Sherlock et al., 1995). The opaline veins locally contain large gold dendrites hosted by fine-grained silica (Fig. 3b). The sheeted vein zone is capped by a siliceous sinter terrace containing interbedded hydrothermal eruption breccia (Fig. 2; Lehrman, 1986).

#### 3. Materials and methods

Detailed fieldwork was performed at McLaughlin to constrain the geology of the deposit and to allow representative sampling of high-grade ores (Sherlock et al., 1995). Opaline vein material investigated in this study was collected from the 1560 S vein. Hand specimen images and chemical maps of the sample material are given by Tharalson et al. (2023).

Following preparation of multiple thin (35–45  $\mu m$ ) sections from the vein material, petrographic investigations in both transmitted and reflected light were conducted using an Olympus BX53 optical microscope. Inspection of the sections under ultraviolet light was performed on the optical microscope using a high-pressure mercury lamp with excitation filtration wavelengths of 330–380 nm. Optical cathodoluminescence microscopy on carbon-coated thin section was conducted using a HC5-LM hot cathode CL microscope by Lumic Special Microscopes, Germany. The instrument was operated at 14 kV and a





Fig. 3. Opaline veins at the McLaughlin deposit. a Multiple generations of cross-cutting veins from the sheeted vein complex. The outcrop image originates from the 1800 level, which is  $\sim\!60$  m below the paleosurface. b Coarse gold dendrite (arrow) hosted by an opaline matrix. The hand specimen was collected on the 1600 bench of the sheeted vein complex, which is  $\sim\!120$  m below the paleosurface. Image modified from Sherlock and Lehrman (1995).

current density of  ${\sim}10~\mu A~mm^{-2}$  (Neuser, 1995). Images were captured with a Teledyne Lumenera Infinity 5–5 digital camera.

Raman spectra on texturally distinct phases were collected using a Horiba LabRAM HR Evolution spectrometer equipped with a 532 nm frequency-doubled Nd:YAG laser (Laser Quantum, Torus 532 + mpc3000) coupled to an Olympus BXFM optical microscope. The laser beam was focused through a 100x objective lens and operated at a 100 % laser power. A 600 lines/mm grating was used. Spectra were collected from 100 to 1500  ${\rm cm}^{-1}$  using a Si-based CCD detector (1024  $\times$  256 pixels). The spectrometer was calibrated using the 520  ${\rm cm}^{-1}$  Raman peak of Si prior to analysis.

#### 4. Results

## 4.1. Noncrystalline silica matrix

Ore minerals in the opaline vein material from McLaughlin are hosted by silica bands that are light tan to amber in color (Fig. 4a, b). The silica bands have variable thicknesses and often exhibit botryoidal and wavy surfaces. The silica bands hosting the ore minerals are composed of relict microspheres that are round and range from  $1-5~\mu m$  in size (Fig. 4b, c). Cavities between the relict microspheres have sickle-like shapes. Variations in packing density of the relict microspheres appear to result in distinct colors of the opaline bands (Fig. 4a, b). The relict microspheres are isotropic in crossed-polarized light (Fig. 4a, b). Raman spectroscopy did not yield descernable peaks due to the strong background luminescence (Fig. 5). Under ultraviolet light excitation, the isotropic silica shows a blue and orange luminescence (Fig. 5c). Based on the isotropic nature and the microspherical texture, the noncrystalline silica forming the opaline bands is classified as opal-A<sub>G</sub> (cf. Smith, 1998).

## 4.2. Incipient recrystallization

The silica in the opaline veins has undergone partial recrystallization in some of the opaline bands. In crossed-polarized light, the silica matrix in these areas is only partly isotropic. High magnification microscopy shows that the relict microspheres vary from spherical with smooth surfaces to spherical or non-spherical consisting of small blade-shaped crystals (Fig. 4c). Based on the textural characteristics, these bladed lepispheres (cf. Wise and Kelts, 1972) consist of opal-CT as shown by Campbell et al. (2001), Lynne and Campbell (2004), Rodgers et al. (2004), Lynne et al. (2005), and Jones (2021).

In many of the opaline bands, incipient recrystallization has resulted in the formation of concentrically banded silica spheres or ovoids, which have a heterogeneous turbid appearance (Fig. 4d). Variations in color between adjacent bands are commonly pronounced in these silica spheres. When near one another, the silica spheres become amalgamated. The concentrically banded silica spheres are isotropic in crossed-polarized light and show luminescence under ultraviolet light (Fig. 5b, c). The absence of discernable Raman peaks (Fig. 5d) and the strong background luminescence may indicate that the concentrically banded silica spheres are still primarily composed of noncrystalline silica. At high magnification, bladed lepispheres can be observed in the concentrically banded silica spheres, suggesting that incipient recrystallization has resulted in the formation of opal-CT.

#### 4.3. Elongated quartz crystals and quartz aggregates

The concentrically banded silica spheres and ovoids may contain elongated quartz crystals that range up to  $\sim 50~\mu m$  in length (Fig. 6a). At low magnification, the quartz crystals appear to be doubly terminated. However, at high magnification it is apparent that the elongated shapes are commonly caused by intergrowth of several smaller quartz crystallites of similar orientation (Fig. 6a). The elongated quartz crystals show well-defined Raman spectra (Fig. 5d). Where the orientation of the

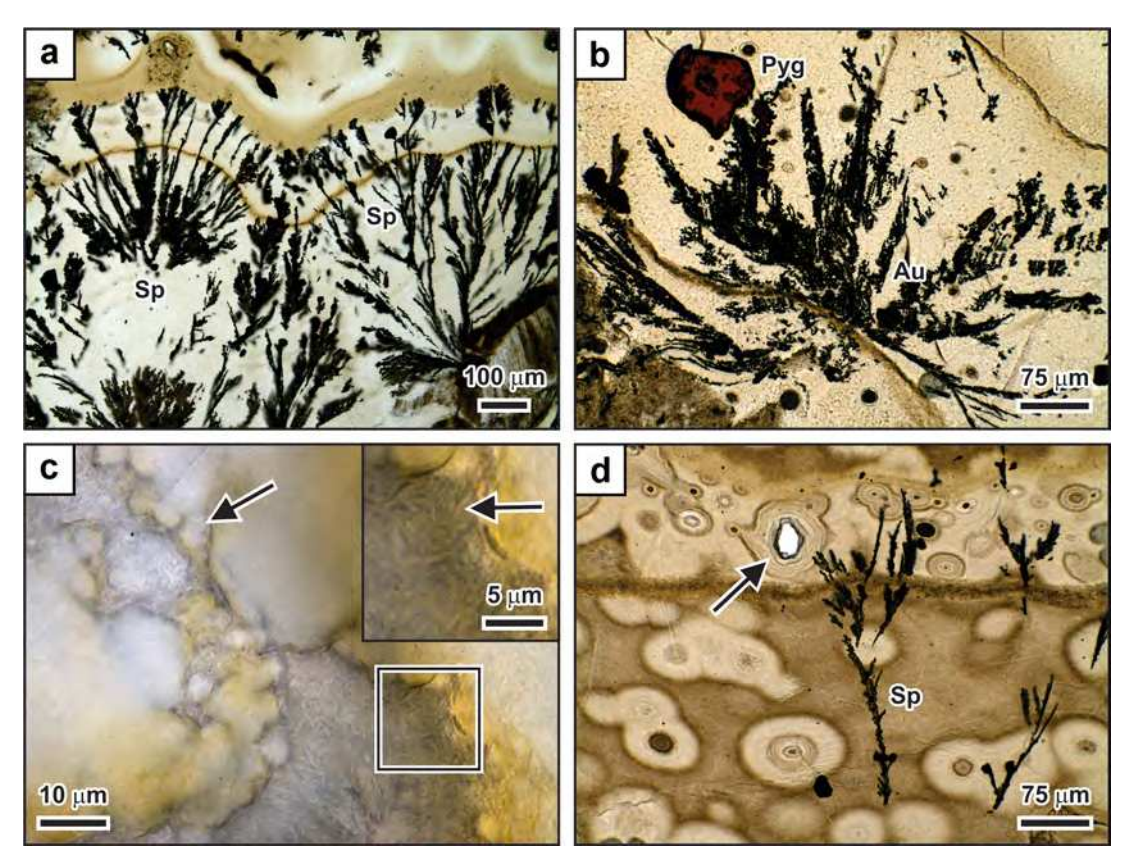


Fig. 4. Noncrystalline silica and incipient recrystallization textures in opaline vein material from the McLaughlin deposit, California. a Opaline silica band hosting delicate sphalerite dendrites that are oriented perpendicular to the botryoidal surfaces. Adjacent opaline bands vary in color. The groundmass of the opaline silica bands is isotropic in crossed-polarized light suggesting that recrystallization of the opaline matrix is limited. b Opaline silica band composed of relict microspheres that hosts a delicate native gold dendrite and a euhedral pyrargyrite crystal. The groundmass has undergone incipient recrystallization as suggested by the presence of small concentrically banded silica spheres. c High-magnification image of the opaline silica. Relict microspheres (arrow) can be clearly identified. The bladed surfaces (arrow in inset) of some of these microspheres suggest that maturation of the originally noncrystalline opal- $A_G$  to opal-CT has already occurred. d Concentrically banded silica spheres and ovoids suspended in the microspherical matrix. Some of the spheres contain quartz crystals in their cores (arrow). The textural relationships suggest that the concentrically banded silica spheres formed during incipient recrystallization of the matrix and postdate the growth of the sphalerite dendrites. All images are plane-polarized light. Abbreviations:  $A_G = A_G = A_G$ 

intergrown quartz crystallites differ, more complexly shaped quartz aggregates are formed (Fig. 6b). In these aggregates, quartz crystallites with subhedral terminations point towards the opaline matrix (Fig. 6b). The texture resembles a row of teeth and is thus referred to as dentine texture in this contribution. In contrast to the elongated quartz crystals, the complexly shaped quartz aggregates are not always surrounded by concentrically banded silica.

#### 4.4. Mosaic quartz

The packing density of elongated quartz crystals is variable and commonly individual crystals in the matrix are randomly oriented. With further maturation, clusters of intergrown quartz crystals occur (Fig. 6c, d). The clusters of quartz crystals exhibit a jigsaw-like geometry with interpenetrating grain boundaries. In crossed-polarized light (Fig. 6d), these clusters show a mosaic extinction pattern as described by Lovering (1972) and Dong et al. (1995). Depending on the degree of recrystallization, the mosaic quartz can be massive or contain small areas of relict microspheres and lepispheres between the newly grown quartz crystals (Fig. 6a, b).

## 4.5. Flamboyant quartz

Recrystallization of the noncrystalline silica matrix also resulted in the development of flamboyant quartz aggregates (Fig. 7). An entire progression of textures can be observed from the small complexly shaped quartz aggregates to circular or oval flamboyant quartz (Fig. 7a, b). The cores of the flamboyant aggregates are typically rich in inclusions and cloudy (Fig. 7c), but the inclusions can also be arranged into radial patterns (Fig. 7b, c). The inclusions are commonly void spaces and appear dark in plane-polarized light. The flamboyant quartz shows a radial extinction pattern in crossed-polarized light (Fig. 7d). The outer margins of the quartz aggregates are irregular or frayed, in many cases forming a dentine texture (Fig. 7c). The density of the flamboyant quartz aggregates is variable. In some opaline bands, these circular to oval quartz aggregates are suspended in the matrix or only locally impinge on each other (Fig. 7b). Where the quartz aggregates are fully amalgamated, mosaic textures may develop. The boundaries between the individual flamboyant quartz aggregates are interpenetrating (Fig. 7e, f).

## 4.6. Prismatic quartz crystals

In some cases, recrystallization of the noncrystalline silica matrix has resulted in the formation of coarse-grained, prismatic quartz crystals. The prismatic quartz frequently forms vein-like zones (Fig. 8a, b) that may occur at high angles to the original banding of the crustiform veins. A progression can be observed from individual flamboyant quartz grains forming within bands of noncrystalline silica to bands of flamboyant quartz grains that have amalgamated (Fig. 8a–d). Continued ripening results in the transformation of flamboyant quartz to prismatic crystals. The largest and most mature prismatic crystals occur in the center of the

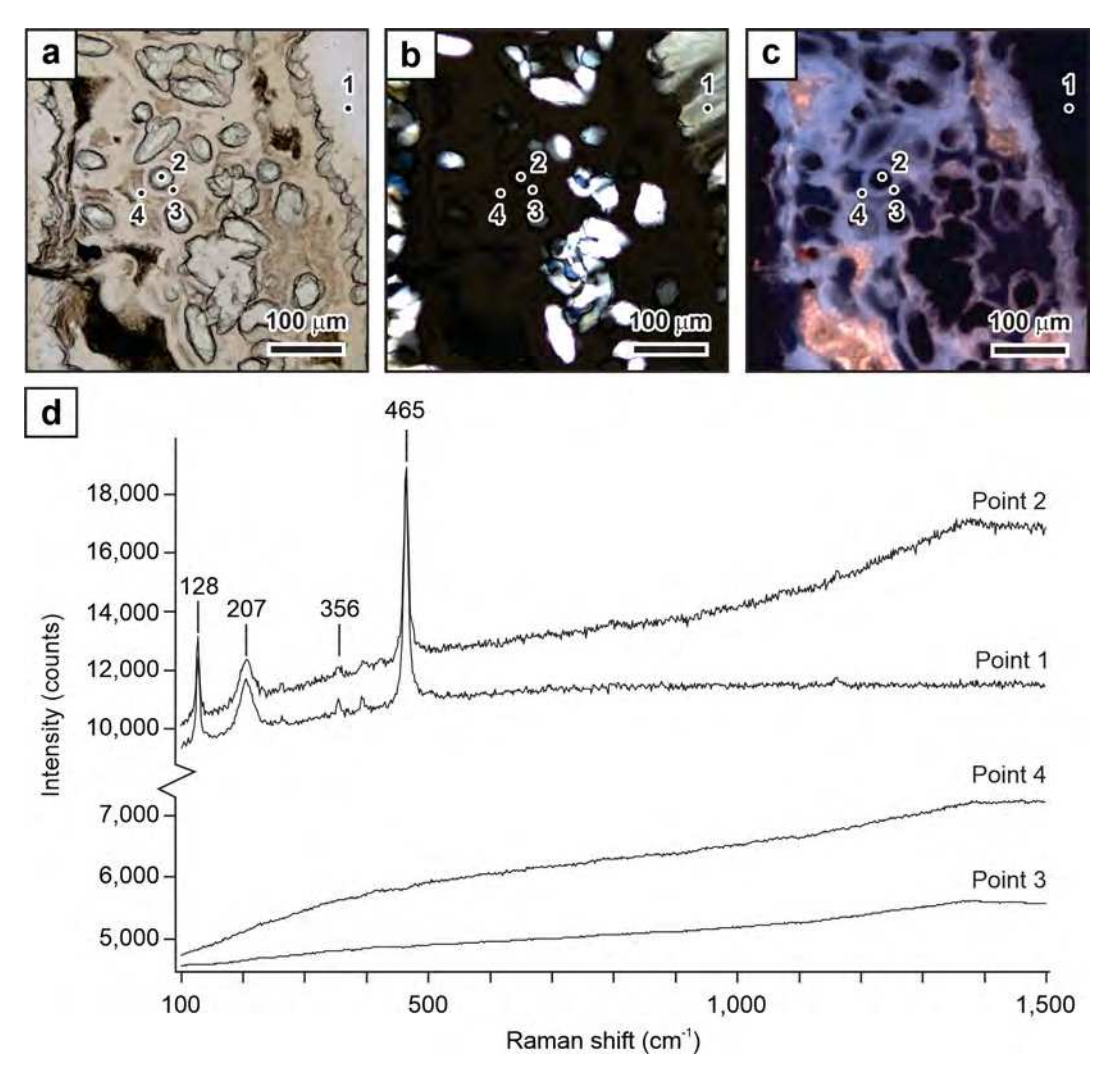


Fig. 5. Partially recrystallized silica matrix in opaline vein material from the McLaughlin deposit, California. a Elongated quartz crystals in noncrystalline silica matrix composed of relict microspheres. The quartz crystals are surrounded by concentrically banded silica spheres. Plane-polarized light, b Crossed-polarized light image of the same field of view illustrating that the silica matrix surrounding the elongated quartz crystals is isotropic. Note that the small quartz crystal suspended in the noncrystalline matrix (spot 2) is extinct as it is viewed down the optical axis. c Luminescent light image of the same field of view collected during ultraviolet light illumination. The noncrystalline silica matrix exhibits a bluish or orange luminescence whereas quartz shows no response, d Raman spectra obtained at the four locations indicated in the images. The quartz shows well-defined spectra whereas the noncrystalline silica matrix is characterized by strong luminescence with no Raman peaks.

vein-like zones whereas smaller grains are present along recrystallization fronts in contact with the opaline matrix (Fig. 8a, b, e, f). Dentine textures suggest that growth of the small quartz crystals along the margins of the vein-like zones occurred outward into the noncrystalline matrix. The degree of maturation and the relative age of the quartz, therefore, decreases from the middle of these vein-like zones outward toward the edges, which is opposite to relationships typically inferred for epithermal veins.

In some cases, the prismatic quartz formed through recrystallization of the noncrystalline silica precursor form vein-like zones consisting of groups of parallel or subparallel crystals that are oriented perpendicular to the banding of the crustiform veins, resembling the comb texture described by Dong et al. (1995). However, similar to recrystallization of flamboyant quartz, these groups of parallel to subparallel quartz crystals did not form in open space (Fig. 9). A sequence of different recrystallization textures is observed. Initially, groups of parallel aligned elongated quartz crystals that are up to  $\sim\!\!50\,\mu\mathrm{m}$  in size are formed within the microspherical matrix (Fig. 9a). Continued maturation results in amalgamation of the elongated crystals forming narrow, vein-like zones in which crystals have similar orientations, as well as the development of

the dentine texture in which quartz crystals on both sides of the vein-like zones point away from the center toward the noncrystalline matrix (Fig. 9b). Zones of larger prismatic crystals form during continued maturation, with the crystals being parallel or subparallel (Fig. 9c). In some zones of recrystallization, large prismatic crystals are present that have euhedral crystal terminations (Fig. 9d).

Prismatic quartz crystals show several characteristics that are inconsistent with growth in open spaces (Fig. 10). Individual crystals appear to have competed for space during recrystallization from the noncrystalline matrix (Fig. 10a, b). Optical cathodoluminescence shows that the large prismatic grains show well-developed zoning patterns, with individual zones ranging from yellow to purple in color (Fig. 10b). The cathodoluminescence emission is short-lived. The colors of the quartz change to dull brown following  $\sim\!60$  s of electron bombardment. The internal zoning patterns are complex. Oscillatory zoning and sector zoning are most pronounced. Individual oscillatory zones are commonly kinked or wavy in nature (Fig. 10b), suggesting that they formed during recrystallization from the noncrystalline silica and are not growth zones that developed in quartz crystals grown in open space. Oscillatory zones can be traced across multiple adjacent quartz crystals that have slightly

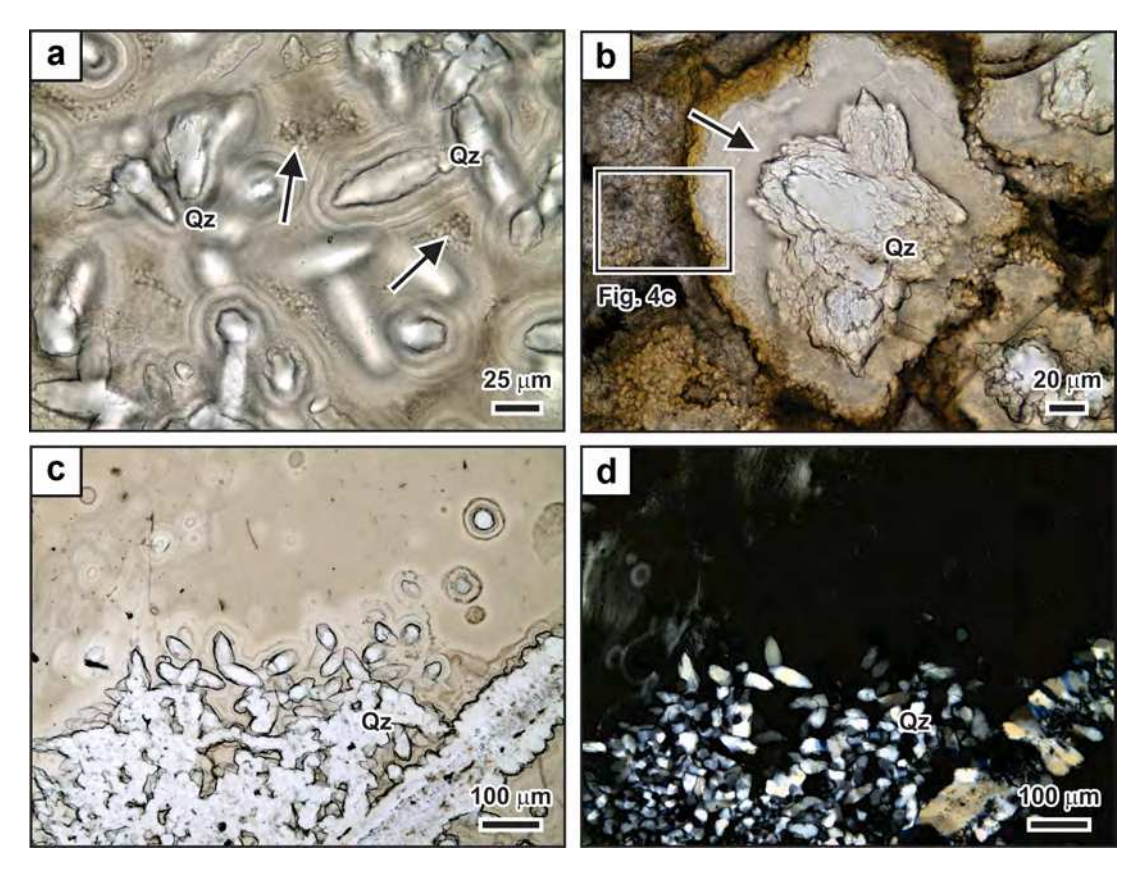


Fig. 6. Recrystallization textures in opaline vein material from the McLaughlin deposit, California. a High-magnification image showing elongated quartz crystals surrounded by concentrically banded silica. Zones containing relict microspheres and lepispheres occur between the areas of concentrical banding (arrows). Plane-polarized light. b High-magnification image of a complexly shaped quartz aggregate showing a dentine texture (arrow). The quartz aggregate is hosted by a non-crystalline silica matrix (see Raman spectrum of point 3 in Fig. 5) surrounded by lepispheres (see high-magnification image in Fig. 4c and Raman spectrum of point 4 in Fig. 5). Plane-polarized light. c Recrystallization of the silica matrix resulted in the development of a mosaic texture through amalgamation of elongated quartz crystals (left). The vein-like zone of quartz crystals (right) exhibits a dentine texture in contact with concentric banding in the noncrystalline silica matrix. Plane-polarized light id Crossed-polarized light image of the same field of view showing that the quartz aggregates within the silica matrix have a mosaic texture where the grain boundaries between the quartz crystals are irregular and interpenetrating. The matrix containing abundant relict microspheres is optically isotropic. Abbreviation: Qz = quartz.

different orientations in crossed-polarized light (Fig. 10a, b).

Prismatic quartz crystals contain abundant inclusions that are commonly distributed along parallel bands (Fig. 10a). These bands resemble growth zones in crystals formed in open spaces. However, the inclusion-rich bands can commonly be traced across several prismatic crystals having different orientations and sizes (Fig. 10a, b). These bands are remnant, crystallographically controlled recrystallization fronts entrapping liquid water originally contained in imperfections between small quartz crystals or along the boundaries between splintery crystallographic domains. Inclusion-rich bands can also be wavy or have rounded edges (Fig. 10c-f). These bands represent remnant recrystallization fronts formed by maturation of the dentine texture that contains abundant imperfections between the small quartz crystals, as evidenced by the dentine texture pointing towards the dark bands of remnant noncrystalline silica located between the prismatic quartz crystals (Fig. 10c, d). As the crystals grow into the matrix, inclusion-rich bands can form along the rims of groups of prismatic crystals competing for space (Fig. 10e, f). The textural evidence is consistent with the inclusionrich bands being remnant recrystallization fronts formed during the transformation of opal-A<sub>G</sub> to quartz, or the continued ripening of the quartz resulting in the formation of the large prismatic crystals.

Many of the prismatic quartz crystals show feathery domains (Fig. 10a, d, f) in which the quartz has a splintery appearance in crossed-polarized light. Individual quartz splinters vary slightly in their extinction positions. Feathery domains can be present in the cores of the prismatic crystals but are most common in rims of grains having clear

cores. Zones of feathery quartz can be continuous to the outer margins of the prismatic quartz crystals. In these cases, the grain boundaries of the large prismatic crystals with the surrounding finer-grained quartz vary from irregular to frayed in nature (Fig. 10f).

## 4.7. Fluid inclusions

The microspherical silica matrix that is anisotropic in crossed-polarized light does not contain fluid inclusions large enough to be identified optically. However, fluid inclusions are present in the different textural types of quartz formed through recrystallization from the noncrystalline precursor.

Flamboyant quartz grains contain abundant inclusions. These are present in dark zones in cores or in dark bands surrounding cores of the grains (Fig. 11a), or form radiating arrays that are typically parallel to the quartz splinters in zones of feathery quartz (Fig. 11b). The textural relationships suggest that these inclusions formed as imperfections in the quartz during recrystallization from the noncrystalline precursor. The inclusions are highly irregular in shape and typically are empty void spaces giving inclusion-rich zones the dark color. In some cases, fluid inclusions containing a liquid and a vapor bubble are present in arrays of empty inclusions (Fig. 11c).

The prismatic quartz crystals may contain abundant bands of pseudoprimary inclusions (Fig. 11d) that were entrapped along crystallographically controlled recrystallization fronts. These inclusions are commonly highly irregular in shape and may be empty void spaces or

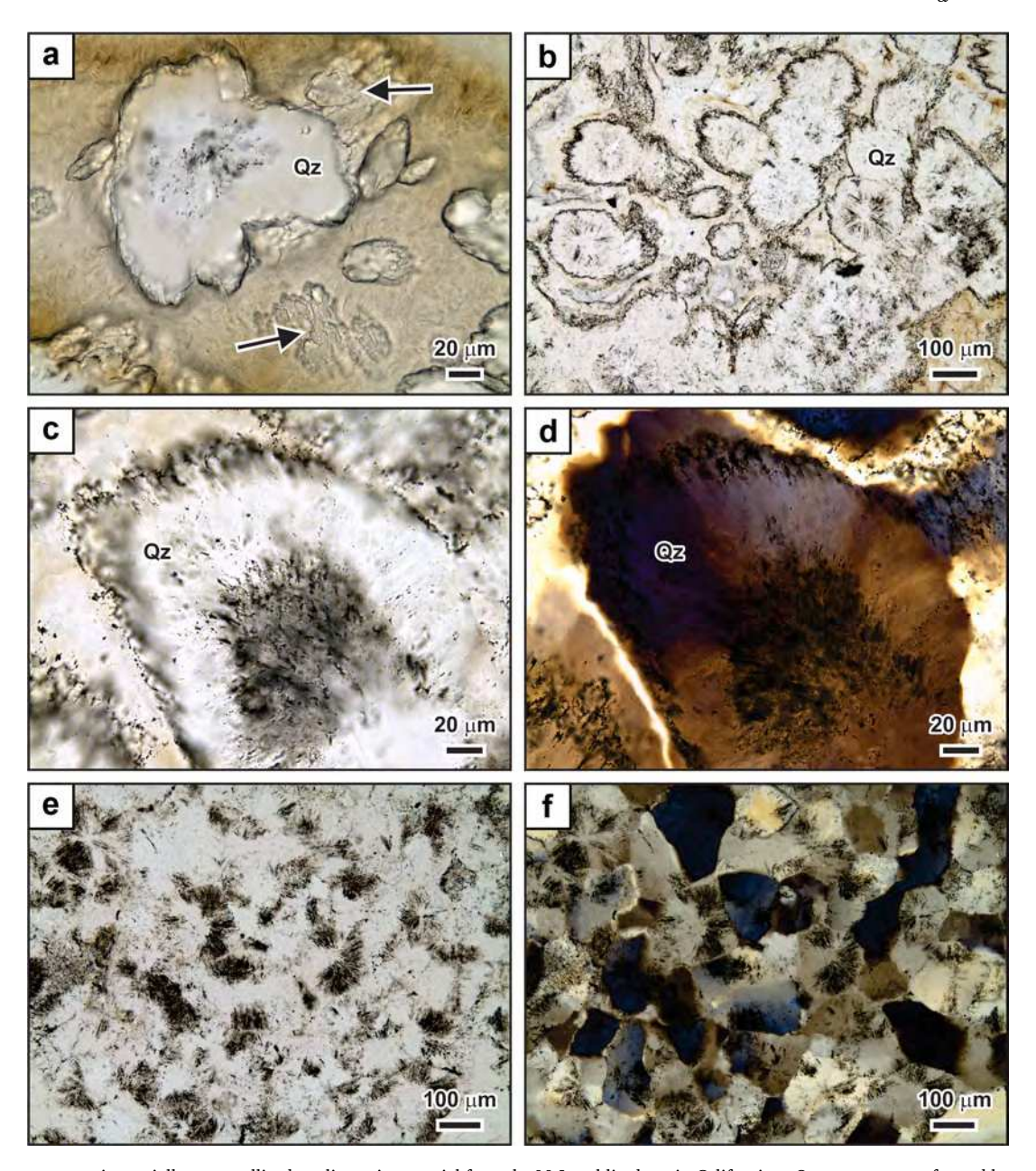


Fig. 7. Flamboyant quartz in partially recrystallized opaline vein material from the McLaughlin deposit, California. a Quartz aggregate formed by amalgamation of quartz crystals growing in different directions in the silica matrix. The core of the aggregate is rich in inclusions. The outer margin of the quartz aggregate shows a dentine texture. The matrix surrounding the large quartz aggregate includes other areas that are recrystallized to quartz (arrows). Plane-polarized light. b Flamboyant quartz aggregates surrounded by a silica matrix. Some of the quartz aggregates contain cores with radially arranged inclusions. The outer margins of the round to elongated quartz aggregates show a dentine texture. Plane-polarized light. c High-magnification image of a flamboyant quartz aggregate showing a dark core of abundant inclusions, with radiating arrays of inclusions present at the margins of the core. The contact between the quartz and the surrounding silica matrix shows a dentine texture. d Partially crossed-polarized light image of the same field of view showing the radial extinction pattern of the flamboyant quartz aggregate. e Aggregate of amalgamated flamboyant quartz grains. Radiating inclusion patterns are locally preserved. f Partially crossed-polarized light image of the same field of view illustrating that the flamboyant quartz grains exhibit interpenetrating grain boundaries. Abbreviation: Qz = quartz.

may have liquid water with or without vapor bubbles, both widely varying in volumetric proportions. Where quartz recrystallization has progressed and inclusions are more mature, the inclusions have equant to negative-crystal shapes and can show consistent liquid-to-vapor volumetric proportions (Fig. 11e). Such fluid inclusions could be mistakenly interpreted as primary fluid inclusions entrapped along growth bands during crystal growth from a hydrothermal fluid.

Large prismatic quartz crystals may contain many secondary fluid inclusion planes. Fluid inclusion assemblages of healed secondary planes can show inconsistent or consistent liquid-to-vapor volumetric proportions. In rare cases, pseudosecondary inclusion planes were observed

suggesting that growth of the prismatic quartz crystals into the surrounding matrix continued after entrapment of the fluid inclusions (Fig. 11f).

#### 4.8. Ore mineral textures

Some of the silica bands in the opaline veins from McLaughlin consisting of opal-A $_{\rm G}$  contain delicate ore mineral dendrites suspended in the noncrystalline silica matrix, including dendrites of sphalerite (Figs. 4a and 12a, b) and native gold (Figs. 4b and 12a, b). The sphalerite dendrites are spinifex-like and are usually oriented perpendicular to the

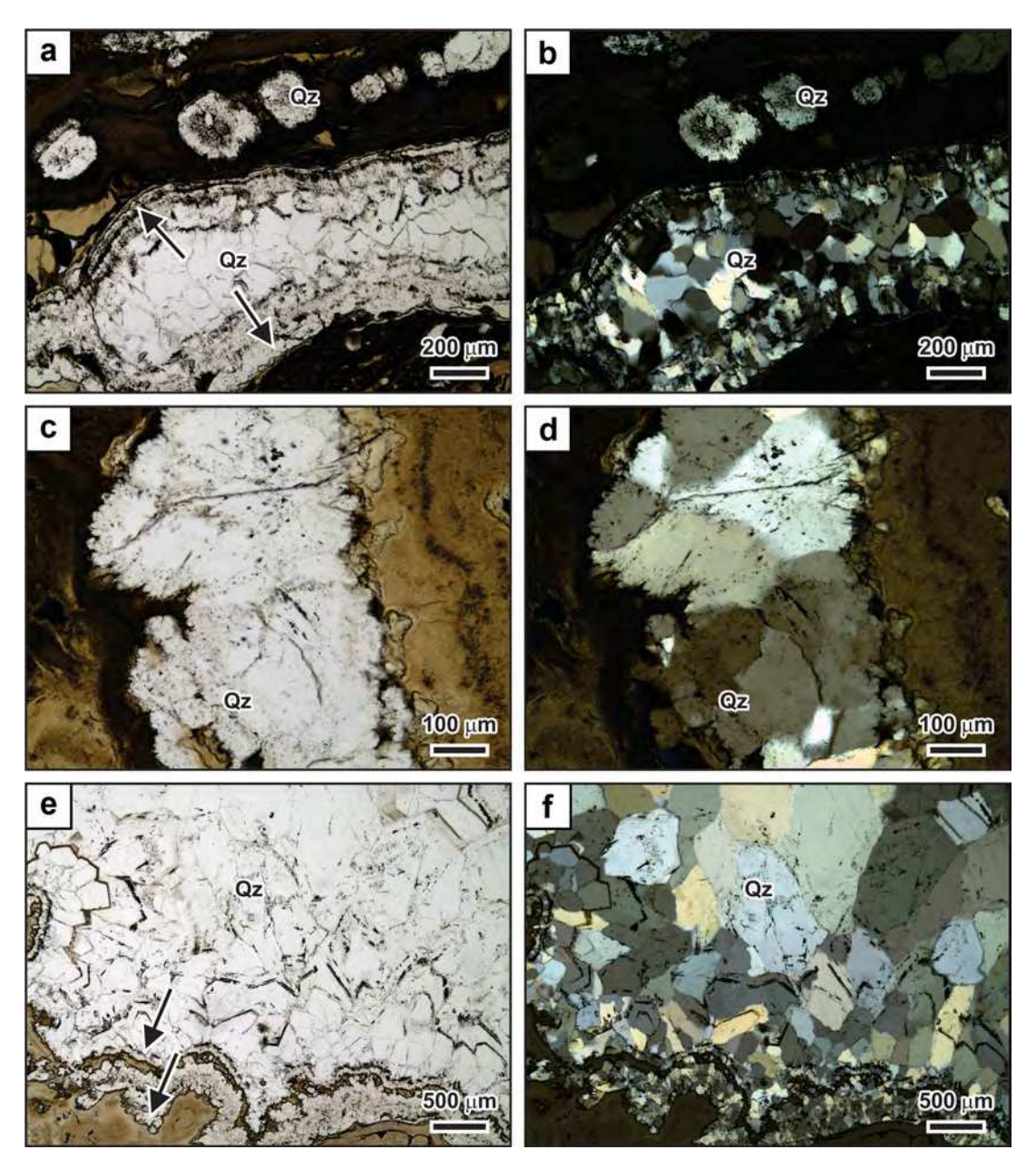


Fig. 8. Prismatic quartz crystals in partially recrystallized opaline vein material from the McLaughlin deposit. a Isolated flamboyant quartz aggregates formed along a band in the opaline vein (upper part of the image). The aggregates grew within the noncrystalline silica matrix. Amalgamation of the quartz aggregates results in a zone of quartz (lower part of the image) that resembles a vein. The contact between the vein-like quartz aggregate and the surrounding matrix has a dentine texture (arrows). Plane-polarized light. b Crossed-polarized light image of the same field of view illustrating that the inner part of the vein-like quartz aggregate formed through recrystallization of the silica matrix is coarser grained than the outer margin where the quartz crystals are close to the surrounding matrix. c High-magnification image of flamboyant quartz aggregates that have formed along a silica band and start to amalgamate. The contact between the quartz and the surrounding matrix is characterized by a dentine texture. Plane-polarized light. d Crossed-polarized light image of the same field of view showing the radial extinction of pattern of the flamboyant quartz. The grain boundaries between the quartz grains are interpenetrating. e Vein-like zone of quartz formed through recrystallization fromts are in the lower part of the picture (arrow) as indicated by the dentine texture. The zone of quartz could be misinterpreted as a crustiform vein formed in open space. Plane-polarized light. f Partially crossed-polarized light image of the same field of view. The grain size of the prismatic quartz is coarsest away from the recrystallization fronts. Abbreviation: Qz = quartz.

colloform banding (Figs. 4a and 12a). Large stubby pyrargyrite crystals occur abundantly in the mineralized silica bands (Figs. 4b and 12a, b).

With recrystallization of the noncrystalline silica matrix, the textural relationships of the ore minerals with the surrounding silica phases are altered, masking the original relationships (Fig. 12c-f). In silica bands that have been affected by recrystallization, the ore mineral dendrites or the pyrargyrite crystals are frequently encased by quartz (Fig. 12c-f). Parts of dendrites or entire dendrites can be encapsulated by a single

quartz crystal or a group of quartz crystals (Fig. 12c, d). Quartz crystals also occur in the matrix between the dendrites (Fig. 12d). Agglomeration results in the formation of quartz aggregates showing a mosaic texture (Fig. 12d). At high magnification, it is apparent that the quartz encapsulating the ore minerals shows a dentine texture in contact with the surrounding matrix, providing textural evidence that the quartz aggregates formed through growth in the matrix (Fig. 12e). The growth of small euhedral crystals surrounding the opaque phases appears to

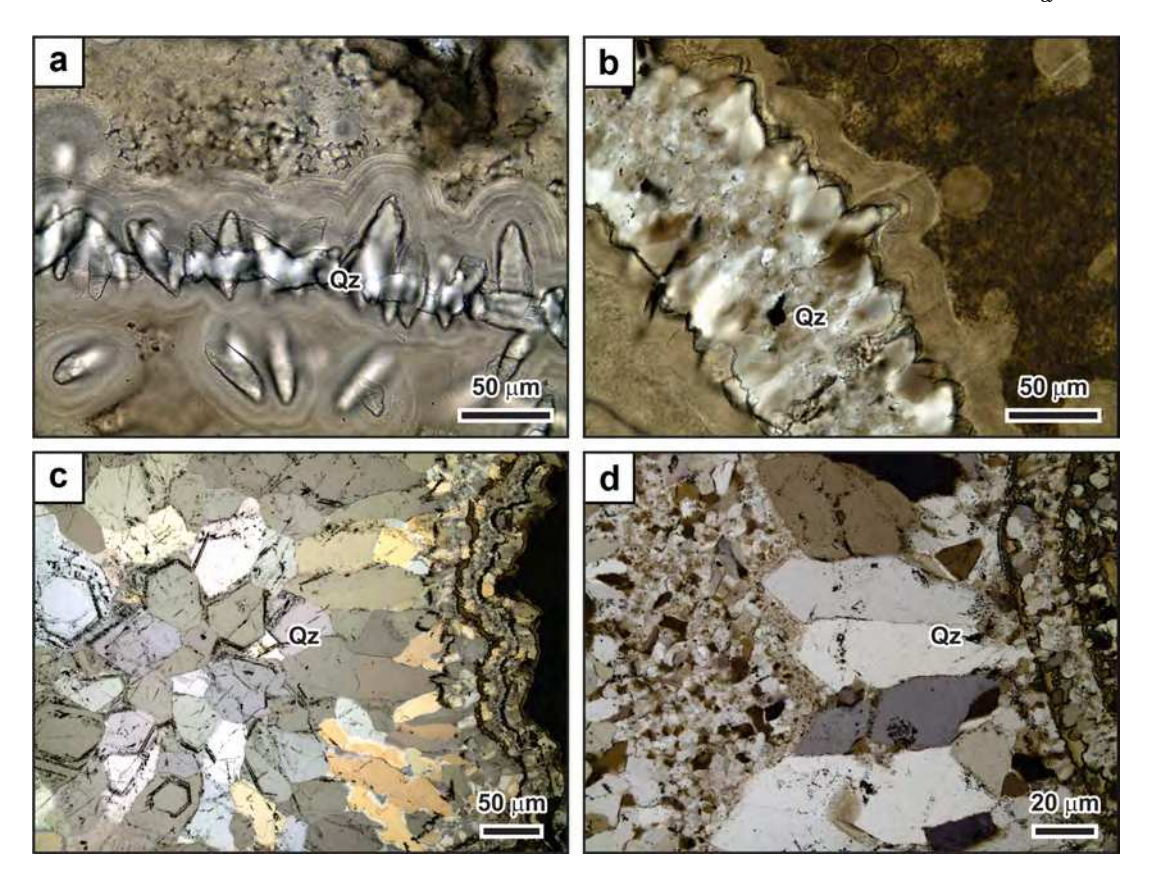


Fig. 9. Aligned prismatic quartz crystals in a partially recrystallized opaline vein material from the McLaughlin deposit. a Small elongated quartz crystals that nucleated and grew in subparallel alignment within the microspherical silica matrix. The quartz crystals are surrounded by concentrically banded silica that is not yet recrystallized to quartz. b Zone of quartz crystals with terminations pointing away from the center of the quartz zone. The dentine texture indicates that the quartz crystals are growing into the surrounding noncrystalline silica matrix. Further maturation will result in a texture that may resemble a vein formed in open space. c Vein-like zone of prismatic quartz crystals formed through recrystallization of the noncrystalline silica precursor. Crystals on the left are more mature and euhedral than those on the right. Some crystals on the right align in a parallel fashion as they competed for space during recrystallization. Small subhedral to anhedral quartz grains occur at the base of large prismatic quartz grains. The quartz is growing to the right as indicated by dentine textures. d Group of prismatic quartz crystals that are parallel and have euhedral crystal terminations. The crystals formed through recrystallization of the noncrystalline silica matrix. All images were taken in partially crossed-polarized light. Abbreviation: Qz = quartz.

have been accompanied by coarsening of the ore mineral grains (Fig. 12c-f). Nucleation and growth of quartz surrounding an ore mineral can yield a texture that could be misinterpreted to represent infilling of a vug by the ore minerals (Fig. 12e, f).

## 5. Discussion

## 5.1. Formation of noncrystalline silica

High-magnification optical microscopy demonstrates that the opaline veins at McLaughlin were originally composed of microspherical silica. The silica matrix in some of the least-recrystallized bands in the opaline veins is still isotropic in nature (Figs. 5a, b and 6c, d), suggesting that this silica phase was noncrystalline at the time of deposition. Raman spectroscopy confirmed that areas of isotropic extinction do not contain quartz (Fig. 5). Following Smith (1998), the microspherical noncrystalline silica at McLaughlin can be classified as opal-A<sub>G</sub>. Saunders (1990) proposed that opal-A<sub>G</sub> was originally gel-like when deposited along the vein walls explaining that bands of opal-A<sub>G</sub> at McLaughlin are often wavy in nature (Fig. 4a), which is most easily explained by hydraulic shaping of the silica.

Ore minerals at McLaughlin form dendrites or euhedral grains within the microspherical silica matrix originally composed of opal- $A_G$  (Figs. 4 and 12). Monecke et al. (2023) hypothesized that the ore minerals grew within the gel-like silica matrix through a diffusion-limited growth process. Textures similar to those observed in the samples from

McLaughlin have been obtained in crystal growth experiments in silica gels (Oaki and Imai, 2003; Monecke et al., 2023). The growth of the ore minerals in a silica gel matrix explains the delicate nature of the ore mineral dendrites and their orientations in the mineralized bands. Although the larger dendrites have nucleated at the base of mineralized bands and appear to have grown towards the top of the bands (Fig. 4a), many smaller dendrites have radiating shapes and appear to have grown in all directions (Fig. 12e, f), which cannot be explained by growth in open space along the vein walls.

## 5.2. Crystallographic changes

The petrographic evidence of this study suggests that the noncrystalline opal- $A_{\rm G}$  forming the opaline veins at McLaughlin has undergone recrystallization to quartz. This maturation process proceeded through a stepwise phase transformation involving the formation of paracrystalline opal-CT which occurs as bladed lepispheres in the samples investigated (Fig. 4c).

The maturation process involving the stepwise conversion of opal- $A_{\rm G}$  to quartz has been studied extensively in the case of silica sinters formed at subaerial hot springs, which are common surface manifestations associated with low-sulfidation epithermal deposits (Sillitoe, 2015). Thermodynamically unstable opal- $A_{\rm G}$  forming young sinter deposits is gradually transformed into quartz through the formation of opal-CT and opal-C (Campbell et al., 2001; Lynne and Campbell, 2004; Rodgers et al., 2004; Lynne et al., 2005; Jones, 2021). Similar recrystallization

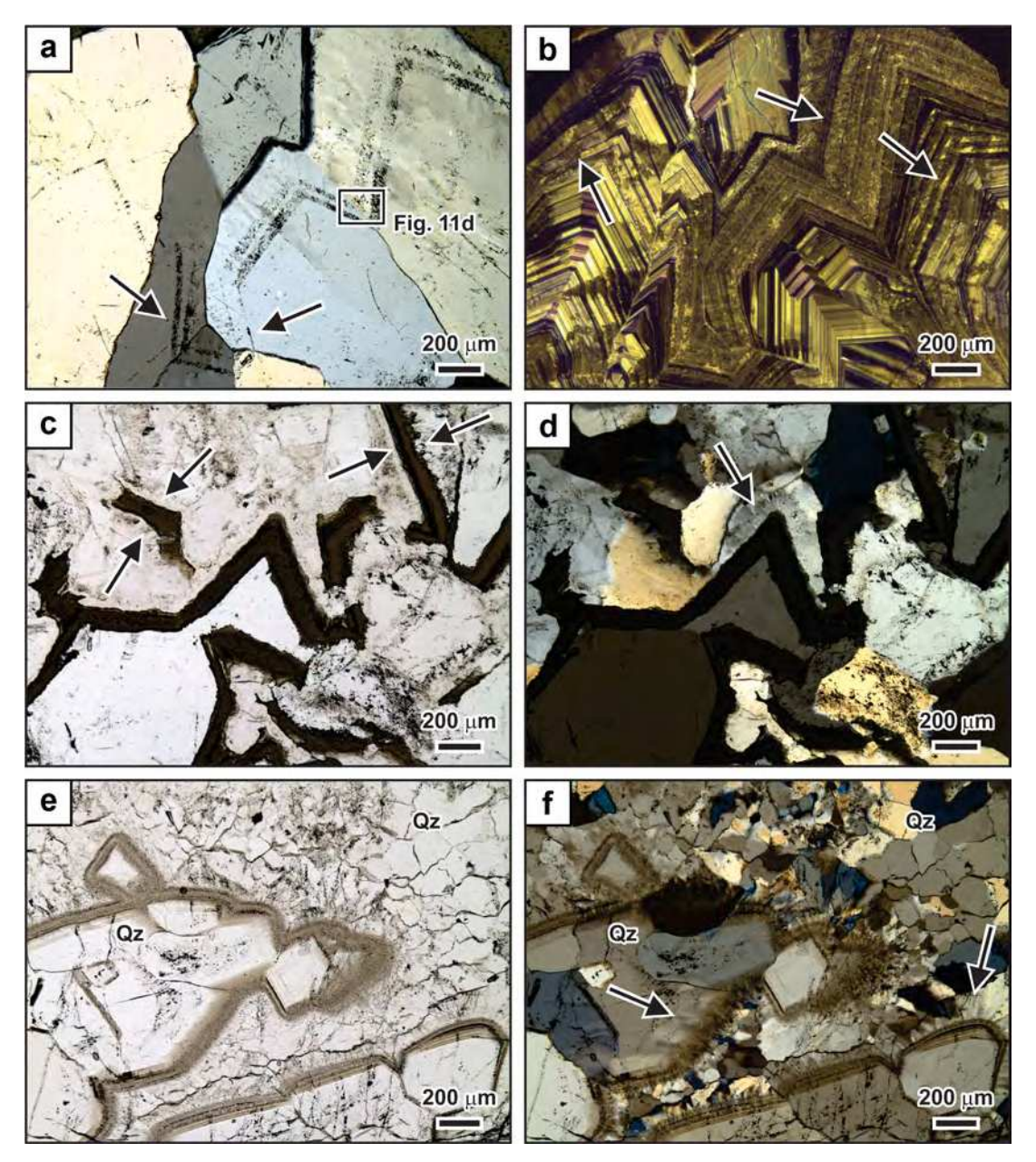


Fig. 10. Prismatic quartz crystals in partially recrystallized opaline vein material from the McLaughlin deposit. a Prismatic quartz crystals formed through recrystallization of a noncrystalline silica precursor. Inclusion bands developed during the recrystallization process are preserved and can be traced across several of the large prismatic crystals that were competing for space during crystal growth (arrows). The prismatic quartz crystals show a feathery texture defined by the presence of quartz splinters that have slightly different extinction positions. Partially crossed-polarized light. b Optical cathodoluminescence image of the same field of view. The prismatic quartz shows pronounced oscillatory zoning. However, the zoning is complicated in detail, with individual zones being kinked or wavy in nature (arrows), confirming that the prismatic quartz formed through recrystallization of a non-crystalline precursor and not through precipitation in open space. c Silica band that is mostly recrystallized to prismatic quartz. The prismatic quartz crystals were competing for space as they grew larger through recrystallization of a noncrystalline silica precursor that is present in the dark brownish bands between crystals (arrows). The contact between the quartz crystals and the silica precursor in the dark bands is characterized by the dentine texture. Plane-polarized light. d Crossed-polarized light image of the same field of view showing that prismatic quartz crystals formed by recrystallization of the noncrystalline silica are competing for space. Zones of feathery quartz are present in some of the crystals (arrow). e Remnant recrystallization fronts in an area that is entirely recrystallized to quartz. The bands defining the remnant recrystallization fronts are rich in inclusions. Plane-polarized light. f Partially crossed-polarized light image of the same field of view. Feathery extinction patterns occur in some of the prismatic quartz crystals or in halos surrounding the crystals (arrows). Abbreviation: Qz

processes involving the formation of opal-CT and opal-C have been documented to occur during the maturation of silica in agate (Götze et al., 2020, 2021) and the diagenesis of siliceous sediments (Murata and Randall, 1975, Hein et al., 1978, Rice et al., 1995). In opal-CT, domains of short-range order are present, while opal-C has more ordered domains (Smith, 1998). Recrystallization occurs through a coupled dissolution-reprecipitation process as described by Williams et al. (1985), Rice

et al. (1995), and Jones and Renaut (2007). Studies on silica sinters have shown that naturally occurring opal- $A_{\rm G}$  recrystallizes to quartz within tens of thousands of years at surface conditions (Herdianita et al., 2000; Rodgers et al., 2004; Lynne et al., 2005). In hydrothermal experiments at temperatures of 300–500 °C, this crystallographic transition has been achieved in as little as days to months (Ernst and Calvert, 1969; Bettermann and Liebau, 1975; Oehler, 1976; Rice et al., 1995).

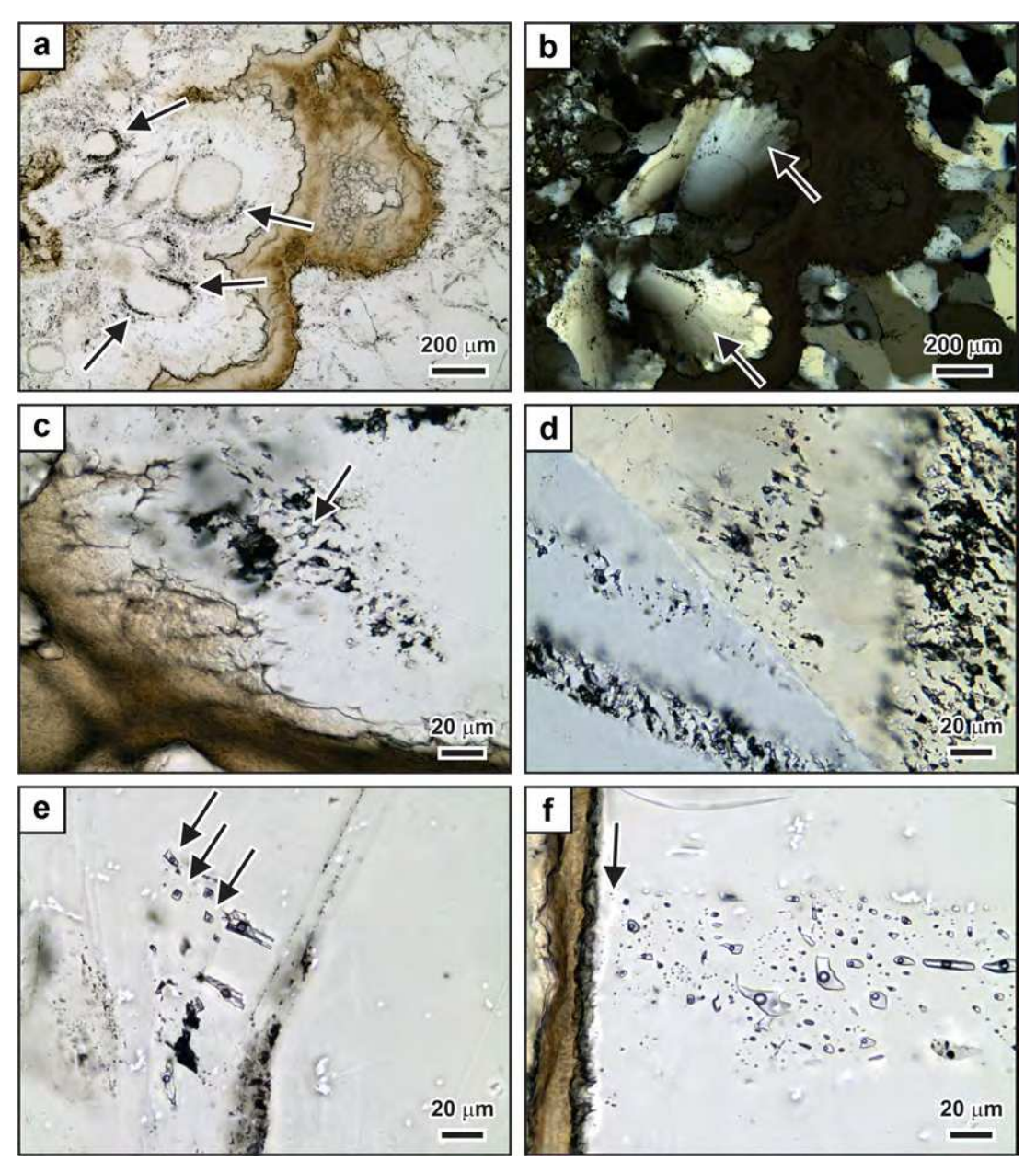


Fig. 11. Fluid inclusion characteristics of quartz formed through recrystallization of the non-crystalline silica in the opaline vein material from the McLaughlin deposit, California. a Flamboyant quartz aggregates surrounded by noncrystalline silica matrix. The quartz in contact with the surrounding matrix has a dentine texture. The flamboyant quartz aggregates are characterized by clear cores that are surrounded by zones that are rich in inclusions (arrows), which are interpreted to represent remnant recrystallization fronts. Plane-polarized light. b Crossed-polarized light image of the same field of view. The outermost zone of the flamboyant quartz aggregate shows a well-developed feathery texture characterized by quartz splinters having slightly different extinction positions. Zones of abundant inclusions occur between the cores of the flamboyant quartz aggregates and the outer zones having a feathery texture. Inclusions are also present between the quartz splinters enhancing the radiating appearance of the quartz aggregate (arrows), c Flamboyant quartz aggregate that shows a dentine texture in contact with the surrounding matrix. The quartz aggregate contains a zone of inclusions that were entrapped during the recrystallization process. The inclusions are highly irregular in shape. Most inclusions are empty void spaces although fluid inclusions are also present (arrow). Plane-polarized light. d Bands of pseudoprimary inclusions that have formed along two, crystallographically controlled, recrystallization fronts that can be traced across several prismatic quartz crystals (see Fig. 10a for location of image). The inclusions are highly irregular in shape. In the outer band, most of the inclusions are empty void spaces. However, in the inner band many of the inclusions are liquid-rich inclusions with a vapor bubble. Plane-polarized light. e Pseudoprimary inclusions with rough to smooth surfaces and elongated, equant, and negative-crystal shapes in a prismatic quartz crystal. Many of the inclusions show consistent liquid-to-vapor volumetric proportions (arrows). Plane-polarized light. f Pseudosecondary fluid inclusion plane crosscutting a larger prismatic quartz crystal. The crystal has formed through recrystallization of the originally noncrystalline silica matrix and is in contact with the matrix on the left side of the photomicrograph. The fluid inclusion plane is truncated by a narrow zone of clear quartz (arrow) suggesting that growth of the prismatic crystal into the matrix continued after healing of the microfracture. The inclusions have smooth surfaces and consistent liquid-to-vapor volumetric proportions. Plane-polarized light.

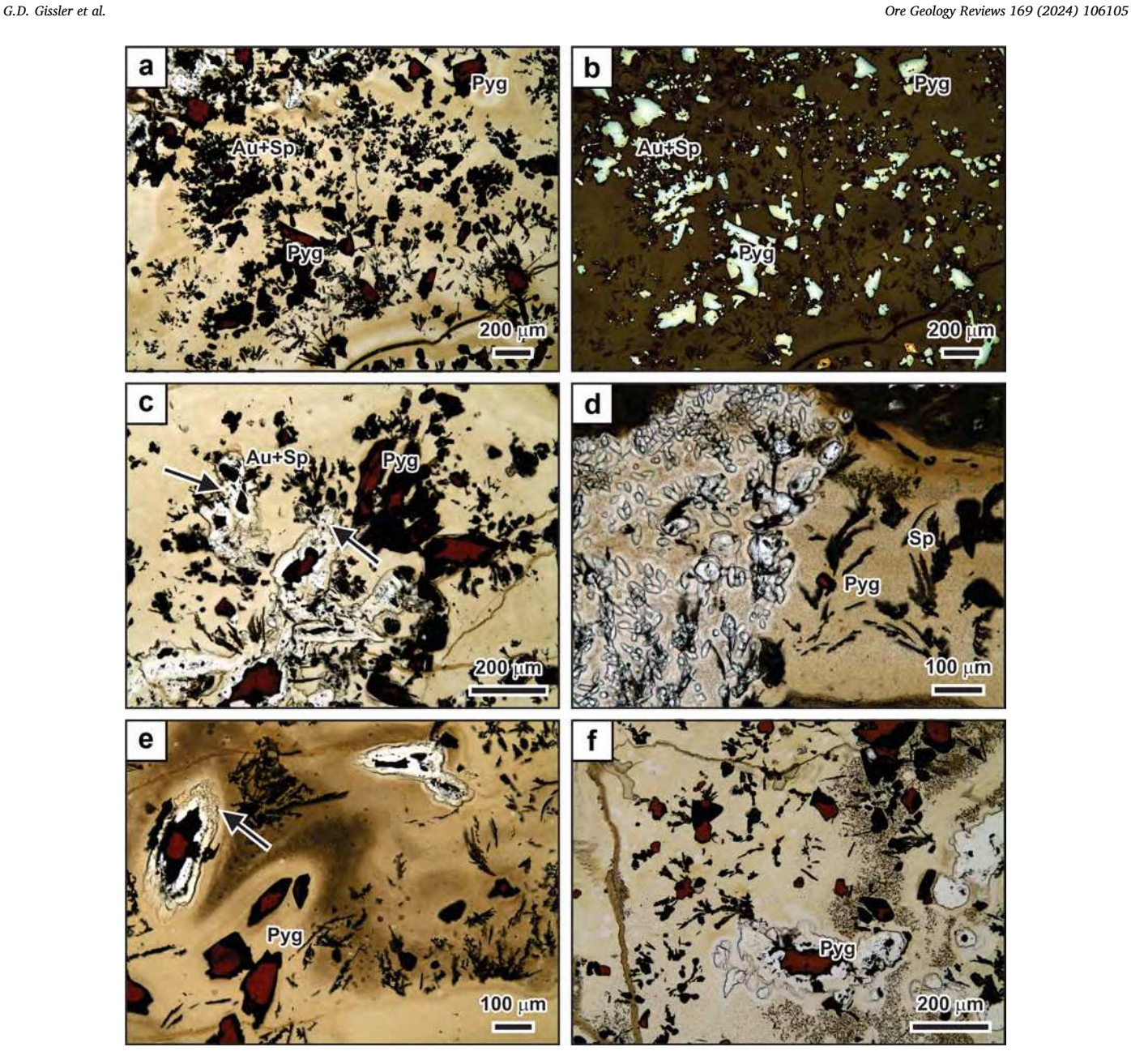


Fig. 12. Ore mineral textures in partially recrystallized opaline vein material from the McLaughlin deposit, California. a Dendrites of native gold and sphalerite set in a matrix consisting of relict silica microspheres. In addition to the dendrites, large euhedral pyrargyrite grains occur. Plane-polarized light. b Reflected light image of the same field of view. The image highlights the abundance of native gold. c Dendrites of native gold and sphalerite as well as euhedral crystals of pyrargyrite in a silica band that shows incipient recrystallization. Some of the ore minerals functioned as nucleation sites for the recrystallization of the noncrystalline silica to quartz. As a result, these are partially encapsulated by quartz (arrows). Plane-polarized light. d Silica band that is partly recrystallized (left side of image). Quartz crystals formed through recrystallization partially or entirely encapsulate the delicate ore mineral dendrites or occur in the silica matrix between the dendrites. Amalgamation of the quartz grains results in the development of quartz aggregates showing a mosaic texture (see Fig. 6c, d) that will host encapsulated ore minerals. Plane-polarized light. e Ore minerals in a partially recrystallized silica band. The ore minerals functioned as nucleation sites for the recrystallization of the noncrystalline silica, with the quartz growing outwards into the matrix as indicated by the presence of the dentine texture (arrow). The color variations in the matrix are a product of recrystallization and not a primary feature caused by the deposition of microspheres of opal-A<sub>G</sub>. Plane-polarized light. f Pyrargyrite and small ore mineral dendrites in a noncrystalline silica matrix that is partially recrystallized. Pyrargyrite in the lower part of the image is encased by quartz crystals formed through recrystallization of the noncrystalline silica precursor. The quartz crystals have grown outward into the silica matrix as indicated by the dentine textures. The resulting textural relationship could be easily misinterpreted as pyrargyrite infilling a vug surrounded by quartz. Abbreviations: Au = native gold, Pyg = pyrargyrite, Sp = sphalerite.

#### 5.3. Textural evolution

Maturation of microspherical opal-A<sub>G</sub> to quartz in sinter deposits is known to be associated with textural changes. The smooth microspheres of opal-A<sub>G</sub> are initially converted to bladed lepispheres of opal-CT (Lynne and Campbell, 2004; Rodgers et al., 2004; Lynne et al., 2005).

During continued recrystallization, the blades on the lepispheres can develop sharp-peaked pyramid or blocky structures, which subsequently recrystallize to quartz microcrystals (Lynne et al., 2005, 2007). Rodgers et al. (2004) demonstrated that small doubly terminated quartz crystals and drusy quartz can form through silica recrystallization in silica sinters originally consisting of opal-A $_{\mbox{\scriptsize G}}$ . Electron microscopic methods were

required to document the microtextural changes accompanying the crystallographic transition from noncrystalline silica to thermodynamically stable quartz due to the small size range of silica microspheres and their recrystallization products.

The study at McLaughlin highlights that recrystallization of opal-A<sub>G</sub> to quartz in epithermal veins results in pronounced textural changes, which can be observed by optical microscopy. Initial maturation of the originally microspherical matrix in the studied opaline veins resulted in the formation of bladed lepispheres composed of opal-CT that can be optically identified at high magnification (Fig. 4c). Concentrically banded silica spheres are formed in the originally noncrystalline silica matrix (Fig. 4d). Continued maturation involves the formation of elongated quartz crystals in the cores of the concentrically banded silica spheres or ovoids and the growth of complexly-shaped quartz aggregates (Fig. 6a, b). As the amount of elongated quartz crystals within the silica matrix increases, mosaic quartz is formed through the amalgamation of the quartz crystals (Fig. 6c, d). The mosaic quartz formed through recrystallization of the opal-A<sub>G</sub> and amalgamation of quartz crystals is characterized by interpenetrating grain boundaries (cf. Dong et al., 1995). Growth of the complexly-shaped quartz crystals results in the development of flamboyant quartz, which is characterized by equant grain shapes and radiating extinction patterns (Fig. 7). As the grain size of the flamboyant quartz crystals increases, the crystals compete for space and develop interpenetrating grain boundaries (Fig. 7e, f). Ripening results in the growth of large prismatic quartz crystals (Figs. 8–10). These crystals show complex internal zoning patterns that may be the result of self-organization occurring during the ripening process (Ortoleva et al., 1994). The yellow optical cathodoluminescence color of the zoned quartz is similar to other types of quartz formed through recrystallization of a noncrystalline silica precursor (Götze et al., 2015).

Some of the opaline bands in the veins of the <2.2 Ma McLaughlin epithermal deposit are almost entirely recrystallized to large prismatic quartz crystals, suggesting that opal- $A_G$  or many of the textures of incipient recrystallization documented in this contribution are unlikely to be preserved in older epithermal deposits. In older epithermal deposits, microspherical opal- $A_G$  that may have been originally present is likely entirely transformed to mosaic quartz, flamboyant quartz, or vein-like prismatic quartz, as originally suggested by Sander and Black (1988).

## 5.4. Timing of fluid inclusion formation

During recrystallization, the noncrystalline opal- $A_G$  originally deposited along the vein walls will have successively lost its water content. Opal- $A_G$  can contain over 10 wt% total  $H_2O$  (Graetsch et al., 1985; Day and Jones, 2008). Water loss during the dissolution-reprecipitation process resulting in the transition from opal- $A_G$  to quartz may result in entrapment of some of the water in microcavities, along grain boundaries, or as microstructural defects in the recrystallizing silica precursor phases (Graetsch et al., 1987; Graetsch, 1994; Moxon, 2017), or within fluid inclusions in the newly formed quartz. At McLaughlin, the fluid inclusion assemblages present in recrystallized quartz commonly show variable liquid-to-vapor volumetric proportions and are thus not suitable for the determination of homogenization temperatures (Fig. 11c,d). Only some assemblages containing consistent phase ratios are present (Fig. 11e, f).

The nature of the fluid inclusions in the recrystallized quartz at McLaughlin is similar to those described by Sander and Black (1988). These authors studied the formation of prismatic quartz crystals in the veins from the Rawhide and Round Mountain low-sulfidation epithermal deposits in Nevada. Sander and Black (1988) suggested that the prismatic quartz crystals in the vein material could have formed due to the recrystallization of a noncrystalline precursor. However, these earlier workers did not document the occurrence of relict microspheres. Sander and Black (1988) proposed that the prismatic quartz crystals

formed through aggregation of microscopic crystallites growing from the noncrystalline precursor and envisaged that submicroscopic to micrometer-sized fluid inclusions were entrapped during aggregation. They proposed that subsequent maturation to progressively coarser prismatic quartz crystals resulted in the coalescence of small fluid inclusions to larger and more regularly shaped inclusions. Sander and Black (1988) referred to these bands as pseudoprimary fluid inclusions, as they formed during recrystallization of a noncrystalline silica precursor and do not reflect the conditions at which the original silica phase was deposited. Pseudoprimary fluid inclusions can be easily mistaken as primary fluid inclusion assemblages entrapped along growth zones in zonal quartz crystals formed in open spaces.

Results of this study on opaline vein material from McLaughlin demonstrate that there are subtle differences between the bands of pseudoprimary fluid inclusions that formed through recrystallization of the noncrystalline silica precursor and growth zones defined by fluid inclusions formed during crystal growth in open spaces (cf. Bodnar et al., 1985). Curved or rounded margins of dark bands of fluid inclusions provide unequivocal evidence for the entrapment of the fluid inclusions along recrystallization fronts (Figs. 8e, f and 10e, f) and indicate that quartz has formed from a noncrystalline silica precursor. Bands of pseudoprimary inclusions that cross grain boundaries of prismatic quartz crystals also provide evidence for quartz formation through recrystallization of a silica precursor (Figs. 10a and 11d).

## 6. Implications

The study at McLaughlin provides an important link between modern geothermal systems where silica scales are mainly composed of noncrystalline opal- $A_G$  (Reyes et al., 2002; Smith et al., 2003; Raymond et al., 2005; Brown, 2011; Taksavasu et al., 2018; van den Heuvel et al., 2018; Chambefort and Stefánsson, 2020) and epithermal veins that are primarily composed of quartz (Dong et al., 1995; Moncada et al., 2012; Shimizu, 2014). The evidence from McLaughlin suggests that silica bands hosting ore minerals were originally composed mainly of a noncrystalline silica precursor that recrystallized to quartz during or after deposit formation.

This study confirms that mosaic quartz is a common product of the recrystallization of the opal-A<sub>G</sub>, which is consistent with previous textural investigations (Taksavasu et al., 2018; Tharalson et al., 2019, 2023; Zeeck et al., 2021). Similarly, flamboyant quartz aggregates and prismatic quartz crystals with zones having a feathery appearance are recrystallization textures resulting from the maturation of opal-A<sub>G</sub> to quartz. Recognition of these quartz textures as products of recrystallization of noncrystalline silica in epithermal veins is of paramount importance when studying the processes that result in precious metal mineralization in shallow hydrothermal systems. In contrast to mineralized bands in colloform epithermal veins that commonly contain quartz showing these textures (Moncada et al., 2012; Shimizu, 2014; Taksavasu et al., 2018; Tharalson et al., 2019, 2023; Zeeck et al., 2021), barren bands show different textural characteristics suggesting that they may not have formed by the same processes. This includes bands composed of chalcedony as well as zonal quartz grown in open space (Moncada et al., 2012; Zeeck et al., 2021).

It is proposed here that mineralized and barren bands in epithermal veins record fundamentally different conditions of fluid flow. Not unlike modern geothermal systems, opal-A<sub>G</sub> deposition in mineralized bands occurred rapidly under conditions of two-phase liquid and vapor flow as silica supersaturation can be readily achieved under these conditions (Fournier, 1985; Saunders, 1990; Simmons and Browne, 2000). The generation of significant amounts of vapor during vigorous boiling results in metal supersaturation in the liquid phase promoting ore deposition (Drummond and Ohmoto, 1985; Brown, 1986; Christenson and Hayba, 1995; Simmons and Browne, 2000). Indeed, sulfide scales in geothermal systems commonly form under these conditions (Raymond et al., 2005; Hardardóttir et al., 2010; Grant et al., 2019). In contrast to

mineral formation during the typically short-lived events of vigorous boiling (cf. Rowland and Simmons, 2012), the formation of barren quartz bands, including growth of zonal quartz in open spaces, records periods of fluid flow at near steady-state conditions. Steady-state fluid flow may have occurred under single-phase conditions or may have been accompanied by the generation of lesser amounts of vapor, referred to as gentle boiling (Moncada et al., 2012).

The present study shows that mineralized silica bands do not contain primary fluid inclusions as they originally consisted of microspherical opal-A<sub>G</sub>. Fluid inclusion bands that mimic growth zones are present in flamboyant and prismatic quartz. However, these pseudoprimary fluid inclusions were entrapped during recrystallization, not at the time of silica and ore mineral deposition as previously noted by Sander and Black (1988). Thus, evidence for vigorous boiling is not found in the fluid inclusion inventory of quartz in mineralized bands. In contrast, zonal quartz—which forms a common late open space infill in the center of epithermal veins-commonly contains primary fluid inclusions (Bodnar et al., 1985; Brathwaite and Faure, 2002; Shimizu, 2014). But these primary inclusions in the late euhedral zonal quartz do not constrain the conditions of ore deposition, as this quartz type was not formed at the same time as the ore minerals that occur in originally noncrystalline silica bands formed during vigorous boiling. Therefore, previous studies drawing conclusions on the processes of ore formation in the epithermal environment based on microthermometric data obtained on quartz formed by recrystallization or late zonal quartz grown in open spaces must be viewed with skepticism.

#### 7. Conclusions

Opaline vein material at the McLaughlin low-sulfidation epithermal deposit was originally composed of mostly noncrystalline, microspherical opal- $A_{\rm G}$ . The opal- $A_{\rm G}$  deposited along the vein walls due to silica oversaturation. Ore mineral dendrites, including native gold, formed within the gel-like silica matrix as suggested by the delicate intergrowth between the ore minerals and the microspherical silica matrix. Growth of the ore mineral dendrites occurred at far-from-equilibrium conditions (Monecke et al., 2023; Tharalson et al., 2023). Following deposition, the noncrystalline silica recrystallized to quartz, resulting in a modification of the original textures.

The study of recrystallization textures at McLaughlin provides the missing link between the primary deposition of opal-AG from hydrothermal liquids in the epithermal environment—which is not unlike the formation of silica scales in geothermal systems—and the fact that most high-grade veins in low-sulfidation epithermal deposits are composed of quartz and not opal-A<sub>G</sub>. The recrystallization of opal-A<sub>G</sub> microspheres to quartz is preserved at McLaughlin. Incipient recrystallization involved the formation of bladed lepispheres composed of opal-CT, followed by the development of concentrically banded silica spheres and ovoids and the growth of elongated quartz crystals and complexly shaped quartz aggregates. Coalescence of these quartz crystals resulted in the formation of mosaic or flamboyant quartz. Ripening of smaller quartz crystals led to the growth of large prismatic quartz crystals, which commonly show feathery internal textures and can host bands of pseudoprimary fluid inclusions, commonly marking remnant recrystallization fronts. Recrystallization and maturation of the matrix can result in the coarsening of the ore minerals, along with complete encapsulation or encasement by quartz crystals.

Processes similar to those recognized at McLaughlin may have occurred at many other epithermal deposits. However, if recrystallization of the original noncrystalline silica to quartz has progressed to completeness, textural evidence for such could be limited to the presence of mosaic quartz, flamboyant quartz, or dark curved bands of remnant recrystallization fronts demarcated by pseudoprimary fluid inclusions. Identification of the products of recrystallization in epithermal quartz veins is critical to investigations aiming to unravel the conditions of mineral precipitation and the design of future fluid

inclusion studies.

#### **Declaration of competing interest**

The authors declare that they have no known competing financial interests or personal relationships that could have appeared to influence the work reported in this paper.

## Data availability

Data will be made available on request.

#### Acknowledgments

Thin section preparation was conducted by S. Dettmar and D. Mann. We thank J. Götze and J. Mauk for comments on an earlier version of the manuscript. The research was financially supported by Colorado School of Mines through a fellowship to G.D.G. provided by Gold Resources Corp. This work was supported in part by the National Science Foundation (NSF) and conducted within the Center to Advance the Science of Exploration to Reclamation in Mining (CASERM), which is a joint industry–university collaborative research center between the Colorado School of Mines and Virginia Tech under the NSF award numbers 2310920 and 2310948. We thank Panagiotis Voudouris and an anonymous reviewer for their constructive reviews of an earlier version of this contribution. Any use of trade, firm, or product names is for descriptive purposes only and does not imply endorsement by the U.S. Government.

#### References

Bettermann, P., Liebau, F., 1975. The transformation of amorphous silica to crystalline silica under hydrothermal conditions. Contrib. Mineral. Petrol. 53, 25–36.

Bodnar, R.J., Reynolds, T.J., Kuehn, C.A., 1985. Fluid-inclusion systematics in epithermal systems. Rev. Econ. Geol. 2, 73–97.

Brathwaite, R.L., Faure, K., 2002. The Waihi epithermal gold-silver-base metal sulfidequartz vein system, New Zealand: Temperature and salinity controls on electrum and sulfide deposition. Econ. Geol. 97, 269–290.

Brown, K.L., 1986. Gold deposition from geothermal discharges in New Zealand. Econ. Geol. 81, 979–983.

Brown, K., 2011. Thermodynamics and kinetics of silica scaling. In: Proceedings of the International Workshop on Mineral Scaling (Manila, Philippines), 8 p.

Campbell, K.A., Sannazzaro, K., Rodgers, K.A., Herdianita, N.R., Browne, P.R.L., 2001.
Sedimentary facies and mineralogy of the late Pleistocene Umukuri silica sinter,
Taupo volcanic zone, New Zealand. J. Sedim. Res. 71, 727–746.

Chambefort, I., Stefánsson, A., 2020. Fluids in geothermal systems. Elements 16, 407–411.

Christenson, B.W., Hayba, D.O., 1995. Hydrothermal eruptions in ore forming reservoirs: analogues and models. In: Proceedings of the PACRIM Congress, Exploring the Rim (Auckland, New Zealand), pp. 119–124.

Day, R., Jones, B., 2008. Variations in water content in opal-A and opal-CT from geyser discharge aprons. J. Sedim. Res. 78, 301–315.

Dong, G., Morrison, G., Jaireth, S., 1995. Quartz textures in epithermal veins,
Queensland—Classification, origin, and implication. Econ. Geol. 90, 1841–1856.

Drummond, S.F., Ohmoto, H. 1985. Chemical evolution and mineral deposition in

Drummond, S.E., Ohmoto, H., 1985. Chemical evolution and mineral deposition in boiling hydrothermal systems. Econ. Geol. 80, 126–147.
 Ernst, W.G., Calvert, S.E., 1969. An experimental study of the recrystallization of

porcelanite and its bearing on the origin of some bedded cherts. Am. J. Sci. 267, 114–133.

Fournier R.O. 1985. The behavior of silica in hydrothermal solutions. Rev. Econ. Geo.

Fournier, R.O., 1985. The behavior of silica in hydrothermal solutions. Rev. Econ. Geol. 2, 45–61.

Götze, J., Pan, Y., Stevens-Kalceff, M., Kempe, U., Müller, A., 2015. Origin and significance of the yellow cathodoluminescence (CL) of quartz. Am. Mineral. 100, 1469–1482.

Götze, J., Möckel, R., Pan, Y., 2020. Mineralogy, geochemistry and genesis of agate – A review. Minerals 10, 1037.

Götze, J., Stanek, K., Orozco, G., Liesegang, M., Mohr-Westheide, T., 2021. Occurrence and distribution of moganite and opal-CT in agates from Paleocene/Eocene tuffs, El Picado (Cuba). Minerals 11, 531.

Graetsch, H., 1994. Structural characteristics of opaline and microcrystalline silica minerals. Rev. Mineral. Geochem. 29, 209–232.

Graetsch, H., Flörke, O.W., Miehe, G., 1985. The nature of water in chalcedony and opal-C from Brazilian agate geodes. Phys. Chem. Minerals 12, 300–306.

Graetsch, H., Flörke, O.W., Miehe, G., 1987. Structural defects in microcrystalline silica. Phys. Chem. Minerals 14, 249–257.

Grant, H.L.J., Hannington, M.D., Hardardóttir, V., Fuchs, S.H., Schumann, D., 2019. Trace metal distributions in sulfide scales of the seawater-dominated Reykjanes

- geothermal system: Constraints on sub-seafloor hydrothermal mineralizing processes and metal fluxes. Ore Geol. Rev. 116, 103145.
- Hardardóttir, V., Hannington, M., Hedenquist, J., Kjarsgaard, I., Hoal, K., 2010. Cu-rich scales in the Reykjanes geothermal system, Iceland. Econ. Geol. 105, 1143–1155.
- Hedenquist, J.W., Arribas, A., Gonzalez-Urien, E., 2000. Exploration for epithermal gold deposits. SEG Rev. 13, 245–277.
- Hein, J.R., Scholl, D.W., Barron, J.A., Jones, M.G., Miller, J., 1978. Diagenesis of late Cenozoic diatomaceous deposits and formation of the bottom simulating reflector in the southern Bering Sea. Sedimentology 25, 155–181.
- Henley, R.W., Brown, K.L., 1985. A practical guide to the thermodynamics of geothermal fluids and hydrothermal ore deposits. Rev. Econ. Geol. 2, 25–44.
- Herdianita, N.R., Browne, P.R.L., Rodgers, K.A., Campbell, K.A., 2000. Mineralogical and textural changes accompanying ageing of silica sinter. Mineral. Deposita 35, 48–62.
- Jones, B., 2021. Siliceous sinters in thermal spring systems: Review of their mineralogy, diagenesis, and fabrics. Sediment. Geol. 413, 105820.
- Jones, B., Renaut, R.W., 2007. Microstructural changes accompanying the opal-A to opal-CT transition: New evidence from the siliceous sinters of Geysir, Haukadalur, Iceland. Sedimentology 54, 921–948.
- Lehrman, N.J., 1986. The McLaughlin mine, Napa and Yolo Counties, California. Nevada Bur. Mines Geol. Rept. 41, 85–89.
- Lipson, R., 2014. The promise and perils of porphyry deposits in the future of gold production. SEG Newsl. 98, 14–21.
- Lovering, T.G., 1972. Jasperoid in the United States—Its characteristics, origin, and economic significance. U.S. Geol. Surv. Prof. Pap. 710, 164 p.
- Lynne, B.Y., Campbell, K.A., 2004. Morphologic and mineralogic transitions from opal-A to opal-CT in low-temperature siliceous sinter diagenesis, Taupo volcanic zone, New Zealand. J. Sediment. Res. 74, 561–579.
- Lynne, B.Y., Campbell, K.A., Moore, J.N., Browne, P.R.L., 2005. Diagenesis of 1900-year-old siliceous sinter (opal-A to quartz) at Opal Mound, Roosevelt Hot Springs, Utah, U.S.A. Sediment. Geol. 179, 249–278.
- Lynne, B.Y., Campbell, K.A., James, B.J., Browne, P.R.L., Moore, J., 2007. Tracking crystallinity in siliceous hot-spring deposits. Am. J. Sci. 307, 612–641.
- Moncada, D., Mutchler, S., Nieto, A., Reynolds, T.J., Rimstidt, J.D., Bodnar, R.J., 2012.
  Mineral textures and fluid inclusion petrography of the epithermal Ag–Au deposits at Guanajuato, Mexico: Application to exploration. J. Geochem. Explor. 114, 20–35.
- Monecke, T., Reynolds, T.J., Taksavasu, T., Tharalson, E.R., Zeeck, L.R., Guzman, M., Gissler, G., Sherlock, R., 2023. Natural growth of gold dendrites within silica gels. Geology 51, 189–192.
- Moxon, T., 2017. A re-examination of water in agate and its bearing on the agate genesis enigma. Mineral. Mag. 81, 1223–1244.
- Murata, K.J., Randall, R.G., 1975. Silica mineralogy and structure of the Monterey Shale, Temblor Range, California. J. Res. U.S. Geol. Surv. 3, 567–572.
- Neuser, R.D., 1995. A new high-intensity cathodoluminescence microscope and its application to weakly luminescing minerals. Bochum. Geol. Geotechn. Arb. 44, 116–118.
- Oaki, Y., Imai, H., 2003. Experimental demonstration for the morphological evolution of crystals grown in gel media. Cryst. Growth Des. 3, 711–716.
- Oehler, J.H., 1976. Hydrothermal crystallization of silica gel. GSA Bull. 87, 1143–1152. Ortoleva, P., Chen, Y., Chen, W., 1994. Agates, geodes, concretions and orbicules: Selforganized zoning and morphology. In: Kruhl, J.H. (Ed.), Fractals and Dynamic Systems in Geosciences. Springer, Berlin, pp. 283–305.
- Raymond, J., Williams-Jones, A.E., Clark, J.R., 2005. Mineralization associated with scale and altered rock and pipe fragments from the Berlin geothermal field, El Salvador; Implications for metal transport in natural systems. J. Volcanol. Geotherm. Res. 145, 81–96.
- Reyes, A.G., Trompetter, W., Britten, K., Searle, J., 2002. Mineral deposits in the Rotokawa geothermal pipelines, New Zealand. J. Volcanol. Geotherm. Res. 119, 215–239
- Rice, S.B., Freund, H., Huang, W.L., Clouse, J.A., Isaacs, C.M., 1995. Application of Fourier transform infrared spectroscopy to silica diagenesis: The opal-A to opal-CT transformation. J. Sediment. Res. 65, 639–647.
- Rodgers, K.A., Browne, P.R.L., Buddle, T.F., Cook, K.L., Greatrex, R.A., Hampton, W.A., Herdianita, N.R., Holland, G.R., Lynne, B.Y., Martin, R., Newton, Z., Pastars, D., Sannazarro, K.L., Teece, C.I.A., 2004. Silica phases in sinters and residues from geothermal fields of New Zealand. Earth Sci. Rev. 66, 1–61.

- Rowland, J.V., Simmons, S.F., 2012. Hydrologic, magmatic, and tectonic controls on hydrothermal flow, Taupo Volcanic Zone, New Zealand: Implications for the formation of epithermal vein deposits. Econ. Geol. 107, 427–457.
- Sander, M.V., Black, J.E., 1988. Crystallization and recrystallization of growth-zoned vein quartz crystals from epithermal systems—Implications for fluid inclusion studies. Econ. Geol. 83, 1052–1060.
- Sanematsu, K., Watanabe, K., Duncan, R.A., Izawa, E., 2006. The history of vein formation determined by <sup>40</sup>Ar/<sup>39</sup>Ar dating of adularia in the Hosen-1 vein at the Hishikari epithermal gold deposit, Japan. Econ. Geol. 101, 685–698.
- Saunders, J.A., 1990. Colloidal transport of gold and silica in epithermal precious-metal systems: Evidence from the Sleeper deposit, Nevada. Geology 18, 757–760.
- Saunders, J.A., 1994. Silica and gold textures in bonanza ores of the Sleeper deposit, Humboldt County, Nevada: Evidence for colloids and implications for epithermal ore-forming processes. Econ. Geol. 89, 628–638.
- Scott, A.M., Watanabe, Y., 1998. "Extreme boiling" model for variable salinity of the Hokko low-sulfidation epithermal Au prospect, southwestern Hokkaido, Japan. Mineral. Deposita 33, 568–578.
- Sherlock, R.L., 2005. The relationship between the McLaughlin gold-mercury deposit and active hydrothermal systems in the Geysers-Clear Lake area, northern Coast Ranges, California. Ore Geol. Rev. 26, 349–382.
- Sherlock, R.L., Lehrman, N.J., 1995. Occurrences of dendritic gold at the McLaughlin mine hot-spring gold deposit. Mineral. Deposita 30, 323–327.
- Sherlock, R.L., Tosdal, R.M., Lehrman, N.J., Graney, J.R., Losh, S., Jowett, E.C., Kesler, S. E., 1995. Origin of the McLaughlin mine sheeted vein complex: Metal zoning, fluid inclusion, and isotopic evidence. Econ. Geol. 90, 2156–2181.
- Shimizu, T., 2014. Reinterpretation of quartz textures in terms of hydrothermal fluid evolution at the Koryu Au-Ag deposit, Japan. Econ. Geol. 109, 2051–2065.
- Sillitoe, R.H., 2015. Epithermal Paleosurfaces. Mineral. Deposita 50, 767-793.
- Simmons, S.F., Browne, P.R.L., 2000. Hydrothermal minerals and precious metals in the Broadlands-Ohaaki geothermal system: Implications for understanding low-sulfidation epithermal environments. Econ. Geol. 95, 971–999.
- Simmons, S.F., White, N.C., John, D.A., 2005. Geological characteristics of epithermal precious and base metal deposits. In: Hedenquist, J.W., Thompson, J.F.H., Goldfarb, R.J., Richards, J.P. (Eds.), Economic Geology 100th Anniversary Volume. Society of Economic Geologists, Littleton, pp. 485–522.
- Smith, D.K., 1998. Opal, cristobalite, and tridymite: Noncrystallinity versus crystallinity, nomenclature of the silica minerals and bibliography. Powder Diffr. 13, 2-19.
- Smith, B.Y., Turner, S.J., Rodgers, K.A., 2003. Opal-A and associated microbes from Wairakei, New Zealand: The first 300 days. Mineral. Mag. 67, 563–579.
- Taksavasu, T., Monecke, T., Reynolds, T.J., 2018. Textural characteristics of noncrystalline silica in sinters and quartz veins: Implications for the formation of bonanza veins in low-sulfidation epithermal deposits. Minerals 8, 331.
- Tharalson, E.R., Monecke, T., Reynolds, T.J., Zeeck, L., Pfaff, K., Kelly, N.M., 2019. The distribution of precious metals in high-grade banded quartz veins from low-sulfidation epithermal deposits: Constraints from µXRF mapping. Minerals 9, 740
- Tharalson, E.R., Taksavasu, T., Monecke, T., Reynolds, T.J., Kelly, N.M., Pfaff, K., Bell, A. S., Sherlock, R., 2023. Textural characteristics of ore mineral dendrites in banded quartz veins from low-sulfidation epithermal deposits: Implications for the formation of bonanza-type precious metal enrichment. Mineral. Deposita 58, 1395–1419.
- Tosdal, R.M., Enderlin, D.A., Nelson, G.G., Lehrman, N.J., 1993. Overview of the McLaughlin precious metal deposit, Napa and Yolo counties, northern California. SEG Guideb. 16, 312–329.
- van den Heuvel, D.B., Gunnlaugsson, E., Gunnarsson, I., Stawski, T.M., Peacock, C.L., Benning, L.G., 2018. Understanding amorphous silica scaling under well-constrained conditions inside geothermal pipelines. Geothermics 76, 231–241.
- Williams, L.A., Parks, G.A., Crerar, D.A., 1985. Silica diagenesis, I. Solubility controls. J. Sediment. Res. 55, 301–311.
- Wise Jr., S.W., Kelts, K.R., 1972. Inferred diagenetic history of a weakly silicified deep sea chalk. Trans. Gulf Coast Assoc. Geol. Soc. 22, 177–203.
- Zeeck, L.R., Monecke, T., Reynolds, T.J., Tharalson, E.R., Pfaff, K., Kelly, N.M., Hennigh, Q.T., 2021. Textural characteristics of barren and mineralized colloform quartz bands at the low-sulfidation epithermal deposits of the Omu Camp in Hokkaido, Japan: Implications for processes resulting in bonanza-grade precious metal enrichment. Econ. Geol. 116, 407–425.